Synthesis and Thermo Gravimetric Analysis of Nickel Filled Carbon Nanotube

A Dissertation submitted towards the partial fulfillment of the requirement for the award of degree of

Master of Technology
in
Nanoscience and Technology

Submitted by

SaurabhTiwari
2K14/NST/13

Under the supervision of

Dr. Pawan Kumar Tyagi
Assistant Professor

Department of Applied Physics
Delhi Technological University
(Formerly Delhi College of Engineering)

JULY 2016

-

दिल्ली प्रोद्योगिकी विश्वविद्यालय
DELHI TECHNOLOGICAL UNIVERSITY
(Formerly Delhi College of Engineering)

CERTIFICATE

This is to certify that the dissertation entitled **"Synthesis and Thermo Gravimetric Analysis of Nickel filled Carbon Nanotube"** submitted to Delhi Technological University (Formerly Delhi College of Engineering) by **Mr. SaurabhTiwari (2K14/NST/13)** in the partial fulfilment of the requirements for the award of the degree of **Master of Technology** in **Nano Science and Technology (Applied Physics Department)** is a bonafide record of the candidate's own work carried out under the supervision of **Dr. Pawan Kumar Tyagi** The information and data enclosed in this thesis is original and has not been submitted elsewhere for honouring any other degree.

Signature of the Candidate

This is to certify that the above statement made by the candidate is correct to the best of my knowledge.

Signature of the Supervisor
Dr. Pawan Kumar Tyagi
(Assistant Professor)
Applied Physics Department
Delhi Technological University
Delhi - 110042

Signature of the HOD
Prof. S. C. Sharma
(Head of Department)
Applied Physics Department
Delhi Technological University
Delhi - 110042

DECLARATION

I hereby declare that all the information in this document has been obtained and presented in accordance with the academic rules and ethical conduct. This report is my own, unaided work. I have fully cited and referenced all material and results that are not original to this work. It is being submitted for the degree of Master of Technology in Nanoscience and Technology at Delhi Technological University. It has not been submitted for any degree or examination in any other university.

Date :

Place:

SaurabhTiwari
M. Tech. NST
2K14/NST/13

ACKNOWLEDGEMENT

I take this opportunity as a privilege to thank all individuals without whose support and guidance, I could not have completed my project successfully in this stipulated period of time.

First and foremost I would like to express my deepest gratitude to my supervisor **Dr. Pawan Kumar Tyagi**, Asst. Professor, Department of Applied Physics, for his invaluable support, Patient guidance, motivation and encouragement throughout the period this work was carried out. I would like to thank **Reetu Singh** and **Lucky Krishnia**, Research Scholar, for valuable time and interest in this project. I am grateful to both for closely monitoring my progress and providing me with timely and important advice, their valued suggestions and inputs during the course of the project work.

I am deeply grateful to **Prof. S.C. Sharma**, H.O.D. (Deptt. of Applied Physics) for his support for providing best educational facilities.

I also wish to express my heart full thanks to the classmates as well as staff at Department of Applied Physics of Delhi Technological University for their goodwill and support that helped me a lot in successful completion of this project.

Finally, I want to thank my parents, brother and friends for always believing in my abilities and for always showering their invaluable love and support.

SaurabhTiwari
M.Tech. NST
2K14/NST/13

TABLE OF CONTENTS

List of Tables

List of figures

Abbreviations used

List Of Figures:

List Of Tables:

List Of Abbreviations:

1. CNT	Carbon Nanotube
2. SWNT	Single Walled Nanotube
3. MWNT	Multi Walled Nanotube
4. Tpa	Tera Pascal
5. AFM	Atomic Force Microscope
6. CVD	Chemical Vapour Deposition
7. H_2	Hydrogen gas
8. CH_4	Methane gas
9. Al_2O_3	Aluminum oxide
10. $MgAl_2O_4$	Magnesium aluminate
11. LCD	Liquid Crystal Display
12. ITO	Indium tin oxide
13. ZnO	Zinc oxide
14. F	Far Ultraviolet
15. FIR	FAR INFRARED
16. FET	Field effect transistor
17. SiO_2	Silicon Oxide
18. VLS	Vapour Liquid Solid
19. CAEM	Controlled atmosphere electron microscope
20. Fe_3C	Iron Carbide
21. HOPG	Highly ordered pyrolytic graphite
22. TGA	Thermo gravimetric analysis
23. DTG	Derivative thermo gravimetric
24. SEM	Scanning electron microscopy
25. TEM	Transmission electron microscopy
26. XRD	X-ray diffraction
27. TA	Thermo Analysis

Chapter 1 Introduction

1.1 Background of Carbon nanotubes :

Carbon nanotubes since their discovery in 1991 by Sumio Iijima, owing to their distinctive electronic and mechanical properties have raised much interest.Their astonishing properties: electrical conduction beyond copper, thermal conduction beyond diamond, tougher than diamond,stronger than steel, etc. Also have generated a huge interest and engendered in numerous potential applications in various fields. Besides these well known applications recently much research interest has been shifted to 3D carbon nano-network, where CNT are connected through either by coating of amorphous carbon or reduced graphene. Recently this network has been envisioned as a superior architecture for lithium ion battery. Further development of carbon based 3D materials include aero-graphite as well as 3D graphene networks have been demonstrated their utilization inflexible magnetic aerogels, stiff magnetic nanopaper, ultra-light and flexible super capacitors electrodes, Li batteries ,conducting composite materials for sensor and photonic applications[28].

1. In order to further explore the applications CNTs possess high thermal stability, high mechanical strength,electrical or thermal conductivity as well as purity are prerequisite. Thus, many research groups have used various methods for the synthesis of CNTs, for example, thermal chemical vapor deposition; plasma enhanced chemical vapor deposition, laser ablation and arc discharge method. But, so far, synthesis of CNTs having quality and purity as needed for specific application is still a challenge. So ,we need a simple method not only for synthesis but also to ensure the purity and quality of carbon nanotubes[29].
2. A carbon nanotube is a tube-shaped material, made of carbon, having a diameter measuring on the nanometer scale. A nanometer is one-billionth of a meter, or about 10,000 times smaller than a human hair. CNT are unique because the bonding between the atoms is very strong and the tubes can have extreme aspect ratios. A carbon nanotube can be as thin as a few nanometers yet be as long as hundreds of microns. To put this into perspective, if your hair had the same aspect ratio, a single strand would be over 40 meters long Carbon nanotubes have many structures, differing in length, thickness, and number of layers. The characteristics of nanotubes

can be different depending on how the graphene sheet has rolled up to form the tube causing it to act either metallic or as a semiconductor. The graphite layer that makes up the nanotube looks like rolled-up chicken wire with a continuous unbroken hexagonal mesh and carbon molecules at the apexes of the hexagons[30].

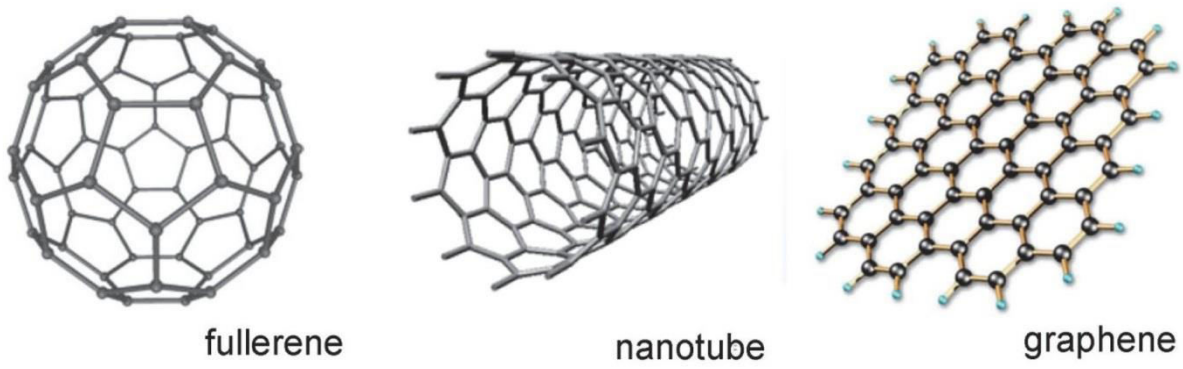

Fig. 1.1: Carbon Structures[26]

1.2Types of Carbon nanotubes :

There are many different types of carbon nanotubes, but they are normally categorized as either single-walled (SWNT) or multi-walled nanotubes (MWNT). A single-walled carbon nanotube is just like a regular straw. It has only one layer, or wall. Multi-walled carbon nanotubes are a collection of nested tubes of continuously increasing diameters. They can range from one outer and one inner tube (a double-walled nanotube) to as many as 100 tubes (walls) or more. Each tube is held at a certain distance from either of its neighboring tubes by interatomic forces.

Single-walled carbon nanotube structure:

Single-walled carbon nanotubes can be formed in three different designs: Armchair, Chiral, and Zigzag. The design depends on the way the graphene is wrapped into a cylinder. For example, imagine rolling a sheet of paper from its corner, which can be considered one design, and a different design can be formed by rolling the paper from its edge. A single-

walled nanotube's structure is represented by a pair of indices (n,m) called the chiral vector[31]. The chiral vector is defined in the image below:

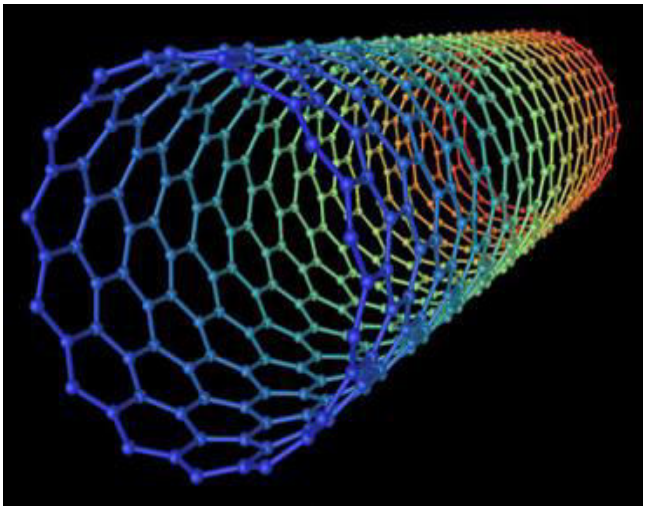

Fig. 1.2: Single walled Carbon nanotube[11]

Multi-walled carbon nanotube structure:

There are two structural models of multi-walled nanotubes. In the Russian Doll model, a carbon nanotube contains another nanotube inside it (the inner nanotube has a smaller diameter than the outer nanotube). In the Parchment model, a single graphene sheet is rolled around itself multiple times, resembling a rolled up scroll of paper. Multi-walled carbon nanotubes have similarproperties to singlewalled nanotubes, yet the outer walls on multi-walled nanotubes can protect the inner carbon nanotubes from chemical interactions with outside materials. Multi-walled nanotubes also have a higher tensile strength than single-walled nanotubes[32].

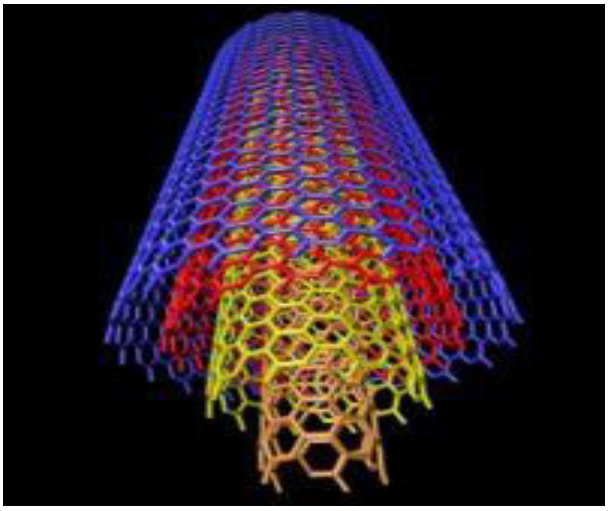

Fig. 1.3: Multi walled Carbon nanotube[11]

It is comparatively easy to think of a single-walled carbon nanotube (SWNT). Ideally, it is sufficient to consider a perfectly formed graphene sheet (graphene is a monoatomic polyaromatic layer comprising of sp2-hybridized carbon atoms that are arranged in hexagons; authentic graphite comprises of layers of this very graphene) and to roll it upto a cylinder such that hexagonal rings placed in contact coherently join. The tips of these tube are sealed by the two caps, whereby each cap being hemi-fullerene of the required diameter. Three unique geometries of the carbon nanotubes are there which are referred to as flavors. These three flavors are zigzag, armchair, and chiral [e.g. zigzag (n,0); armchair (n, n); as well as chiral (n, m)][33]. These details can be easily comprehended by the help of the figures below:

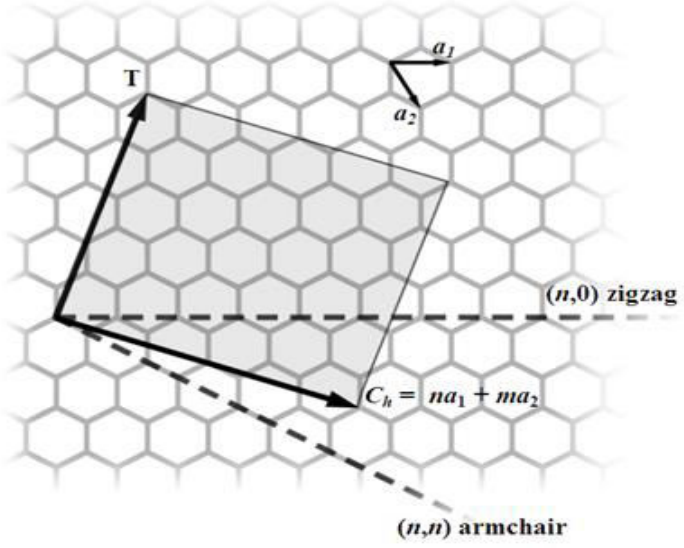

The structural design has a direct effect on the nanotube's electrical properties. When n − m is a multiple of 3, then the nanotube is described as "metallic" (highly conducting), otherwise the nanotube is a semiconductor. The Armchair design is always metallic while other designs can make the nanotube a semiconductor.

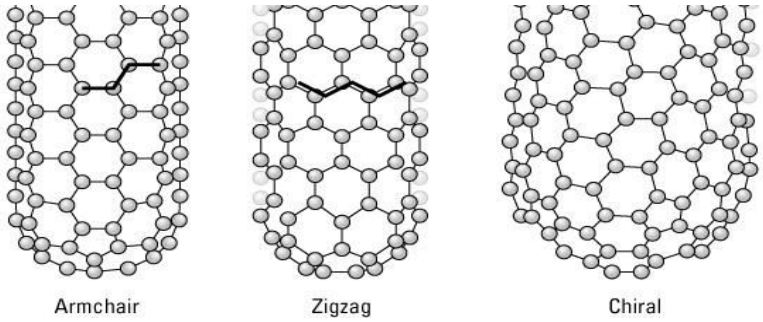

Fig. 1.4: Structural designs of Carbon nanotube[23]

By geometry, there is no restrain on the diameter of the tube. But calculations have indicated that collapsing this single-wall tubular structure into a flattened two-layered ribbon is energetically more favorable than to maintain this tubular morphology beyond a particular diameter value of about 2.5nm.On the other hand, it is well deducible that the shorter the radius of curvature is, the higher the energetic cost and the stress becomes, even though SWNTs having diameters as small as 0.4 nm have been already synthesized successfully. Therefore, the suitable energetic compromise is reached for about 1.4nm, the most repeated diameter encountered irrespective of the synthesis technique when the conditions which ensure high SWNT yields are utilized. There is no restrain on nanotube length, that depends only on the limitations of the method of preparation and the specific conditions that are used for the synthesis (residence time, thermal gradients, and so on). Experimental data are found to be consistent with these statements, since these SWNTs wider than 2.5 nm are only rarely reported in the literature, whatever the preparation method, while the length of the SWNTs can be in the micrometer or the millimeter range. These special features make these single-wall carbon nanotubes an extremely unique example of single molecules possessing huge aspect ratios.

Two important consequences derive from the SWNT structure as described above:

1. All the carbon atoms are involved in the hexagonal aromatic rings only and therefore are in equivalent positions, but except at each and every nanotube tip, where 6 × 5 = 30 atoms are found to be involved in pentagonal ring (considering that the adjacent pentagons are quite unlikely) – though neither more, nor less, as the consequence of Euler's rule which also governs the structure of fullerene. For ideal SWNTs, the chemical reactivity will thereby, be highly favored at tube tips, at the pentagonal rings[34].

2. Although carbon atoms are found to be involved in the aromatic rings, the C=C bond angles are however not planar. This implies that the hybridization of those carbon atoms is certainly not pure sp^2; it does possess some degree of the sp^3 character, which is in inverse proportion to that tube radius of curvature. The effect is similar for C60 fullerene molecules, wherein the radius of curvature is 0.35 nm, and therefore whose bonds have 10% sp3 character. This is believed, on the one hand, to make SWNT surface somewhat more reactive than the regular and planar graphene, in spite of it still consisting of aromatic ring faces. This somehow induces the variable overlapping of the energy bands, which results in versatile and unique electronic behavior. As illustrated by the above figure, there are multiple ways to roll a graphene into a single-walled nanotube, with some of the resultant nanotubes exhibiting planes of symmetry, both parallel as well as perpendicular to the nanotube axis. Just like the terms used for the molecules, the latter are commonly termed as *chiral* nanotubes, since they are not able to be superimposed on their very own image in a mirror. The various ways in order to roll graphene into tubes are thereby mathematically defined by vector of the helicity$\boldsymbol{C}$h, and angle of helicityθ[35].

1.3 Properties of Carbon nanotubes:

1.3.1 Electrical Conductivity: CNTs can be highly conducting, and hence can be said to be metallic. Their conductivity has been shown to be a function of their chirality, the degree of twist as well as their diameter. CNTs can be either metallic or semi-conducting in their electrical behavior. Conductivity in MWNTs is quite complex. Some types of "armchair"-structured CNTs appear to conduct better than other metallic CNTs. Furthermore, inter-wall reactions within multi walled nanotubes have been found to redistribute the current over individual tubes non-uniformly. However, there is no change in current across different parts of metallic single-walled nanotubes. The behavior of the ropes of semi-conducting single

walled nanotubes is different, in that the transport current changes abruptly at various positions on the CNTs.

The conductivity and resistivity of ropes of single walled nanotubes has been measured by placing electrodes at different parts of the CNTs. The resistivity of the single walled nanotubes ropes was of the order of 10–4 ohm-cm at 27°C. This means that single walled nanotube ropes are the most conductive carbon fibers known. The current density that was possible to achieve was 10-7 A/cm^2, however in theory the single walled nanotube ropes should be able to sustain much higher stable current densities, as high as 10-13 A/cm^2. It has been reported that individual single walled nanotubes may contain defects. Fortuitously, these defects allow the single walled nanotubes to act as transistors. Likewise, joining CNTs together may form transistor-like devices. A nanotube with a natural junction (where a straight metallic section is joined to a chiral semiconducting section) behaves as a rectifying diode – that is, a half-transistor in a single molecule. It has also recently been reported that single walled nanotubes can route electrical signals at speeds up to 10 GHz when used as interconnects on semi-conducting devices[36].

1.3.2 Strength and Elasticity: The carbon atoms of a single sheet of graphite form a planar honeycomb lattice, in which each atom is connected via a strong chemical bond to three neighboring atoms. Because of these strong bonds, the basal plane elastic modulus of graphite is one of the largest of any known material. For this reason, CNTs are expected to be the ultimate high-strength fibers. Single walled nanotubes are stiffer than steel, and are very resistant to damage from physical forces. Pressing on the tip of a nanotube will cause it to bend, but without damage to the tip. When the force is removed, the nanotube returns to its original state. This property makes CNTs very useful as probe tips for very high-resolution scanning probe microscopy. Quantifying these effects has been rather difficult, and an exact numerical value has not been agreed upon. Using atomic force microscopy, the unanchored ends of a freestanding nanotube can be pushed out of their equilibrium position, and the force required to push the nanotube can be measured. The current Young's modulus value of single walled nanotubes is about 1 Tera Pascal, but this value has been widely disputed, and a value as high as 1.8 Tpa has been reported. Other values significantly higher than that have also been reported. The differences probably arise through different experimental measurement techniques. Others have shown theoretically that the Young's modulus depends on the size and chirality of the single walled nanotubes, ranging from 1.22 Tpa to 1.26 Tpa. They have

calculated a value of 1.09 Tpa for a generic nanotube. However, when working with different multi walled nanotubes, others have noted that the modulus measurements of multi walled nanotubes using AFM techniques do not strongly depend on the diameter. Instead, they argue that the modulus of the multi walled nanotubes correlates to the amount of disorder in the nanotube walls. Not surprisingly, when multi walled nanotubes break, the outermost layers break first[36].

1.3.3 Thermal Conductivity and Expansion:

CNTs have been shown to exhibit superconductivity below 20°K (approx. -253°C). Research suggests that these exotic strands, already heralded for their unparalleled strength and unique ability to adopt the electrical properties of either semiconductors or perfect metals, may someday also find applications as miniature heat conduits in a host of devices and materials. The strong in-plane graphitic carbon - carbon bonds make them exceptionally strong and stiff against axial strains. The almost zero in-plane thermal expansion but large inter-plane expansion of single walled nanotubes implies strong in-plane coupling and high flexibility against non-axial strains.

Many applications of CNTs, such as in nanoscale molecular electronics, sensing and actuating devices, or as reinforcing additive fibers in functional composite materials, have been proposed. Reports of several recent experiments on the preparation and mechanical characterization of CNT-polymer composites have also appeared. These measurements suggest modest enhancements in strength characteristics of CNT-embedded matrixes as compared to bare polymer matrixes. Preliminary experiments and simulation studies on the thermal properties of CNTs show very high thermal conductivity. It is expected, therefore, that nanotube reinforcements in polymeric materials may also significantly improve the thermal and thermo-mechanical properties of the composites[36].

1.3.4 Field Emission**:** Field emission results from the tunneling of electrons from a metal tip into vacuum, under application of a strong electric field. The small diameter and high aspect ratio of CNTs is very favorable for field emission. Even for moderate voltages, a strong electric field develops at the free end of supported CNTs because of their sharpness. This was observed by de Heer and co-workers at EPFL in 1995. He also immediately realized that these field emitters must be superior to conventional electron sources and might find

their way into all kind of applications, most importantly flat-panel displays. It is remarkable that after only five years Samsung actually realized a very bright color display, which will be shortly commercialized using this technology. Studying the field emission properties of multi walled nanotubes, Bonard and co-workers at EPFL observed that together with electrons, light is emitted as well. This luminescence is induced by the electron field emission, since it is not detected without applied potential. This light emission occurs in the visible part of the spectrum, and can sometimes be seen with the naked eye[36].

1.3.5 High Aspect Ratio:

CNTs represent a very small, high aspect ratio conductive additive for plastics of all types. Their high aspect ratio means that a lower loading of CNTs is needed compared to other conductive additives to achieve the same electrical conductivity. This low loading preserves more of the polymer resins' toughness, especially at low temperatures, as well as maintaining other key performance properties of the matrix resin. CNTs have proven to be an excellent additive to impart electrical conductivity in plastics. Their high aspect ratio, about 1000:1 imparts electrical conductivity at lower loadings, compared to conventional additive materials such as carbon black, chopped carbon fiber, or stainless steel fiber[36].

1.3.6 Highly Absorbent:

The large surface area and high absorbency of CNTs make them ideal candidates for use in air, gas, and water filtration. A lot of research is being done in replacing activated charcoal with CNTs in certain ultra high purity applications[36].

1.4 Synthesis methods for Carbon nanotubes:

A number of methods are used to produce CNTs. In earlier days, carbon combustion and vapor deposition processes were used to produce CNTs. Using the earlier method (plasma arcing) of producing CNTs in reasonable quantities, an electric current was applied across two carbonaceous electrodes in an inert gas atmosphere. The plasma arcing method is primarily used to produce CNTs from different carbonaceous materials such as graphite. The CNTs are deposited on the electrode. Plasma arcing method can also be applied in the

presence of cobalt with 3 % or greater concentration. Different methods for production of CNTs are discussed below:

1.4.1 Arc Discharge Method: The most common and easiest way to produce CNTs is the carbon arc discharge method. Using this method, a complex mixture of components is produced that separates the CNTs from soot and the catalytic metals. Arc vaporization is used to produce CNTs by placing two carbon rods from end to end, separated by an approximate distance of 1 mm, placed in an enclosure. At low pressure, the enclosure is usually filled with inert gas. A high temperature discharge between two electrodes is created by applying a direct current of 50 to 100 A. The surface of the carbon electrodes is vaporized by the high temperature discharge and finally forms a small rod-shaped electrode. The production of CNTs in high yield primarily depends on the uniformity of the plasma arc. The arc discharge method with liquid nitrogen can also be used to produce CNTs[37].

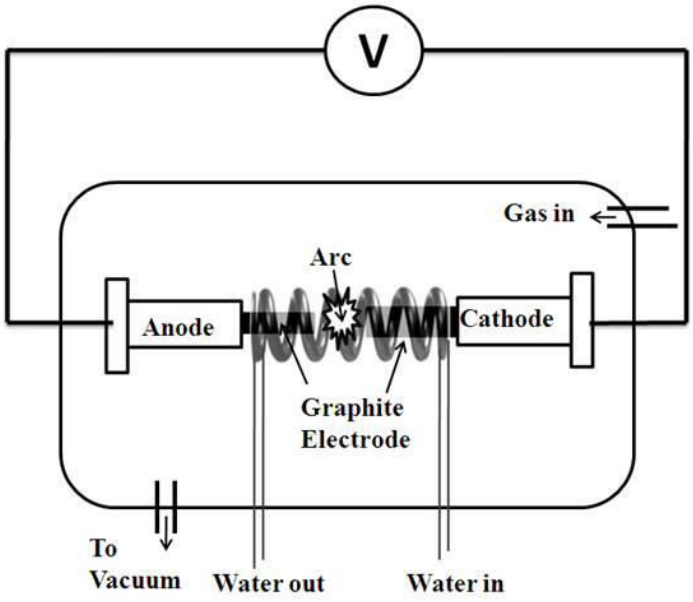

Fig. 1.5: Schematic diagram of Arc discharge[18]

1.4.2 Laser ablation Method: In 1996, a dual-pulsed laser was used in synthesis techniques for producing CNTs with 70 % purity. Presently the laser vaporization process is used for producing CNTs. In this process, a graphite rod with 50:50 catalyst mixtures of cobalt and nickel at 1200 °C in flowing argon is used to prepare the sample (Ahmed 2010). The uniform vaporization of the target can be achieved by using the initial laser vaporization

pulse followed by a second pulse. The amount of deposition of carbon as soot is primarily minimized by the usage of these two successive laser pulses. The larger particles are broken by applying the second laser pulse. The CNTs produced through this process are 10–20 nm in diameter and 100 μm or more in length. The average nanotube diameter and size distribution can vary for different growth temperature, catalyst composition, and other process parameters. In recent years, the arc discharge and laser vaporization methods are used to obtain high quality CNTs in small quantity.

However, above both methods suffer from the following two drawbacks:

(1) The methods use the evaporation of carbon source that follows an unclear approach to scale up the production with industrial standard.

(2) The CNTs produced by vaporization method get mixed with residues of carbon. Therefore, it is quite difficult to purify, manipulate, and assemble CNTs for building nanotube device architectures for practical applications[38].

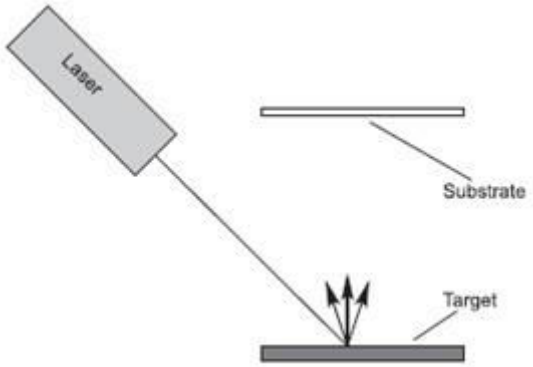

Fig. 1.6: Schematic diagram of Laser ablation[19]

1.4.3 Ball Milling: One of the simple methods for the production of CNTs is through ball milling followed by subsequent annealing. Thermal annealing is used to produce CNTs from carbon and boron nitride powder. In this method, graphite powder is placed in a stainless steel container consisting of four hardened steel balls. The steel container is purged, and argon is introduced for milling process, at room temperature, for up to 150 hour. Using the milling process, the annealing of graphite powder is carried out under an inert gas flow at 1400 ºC for 6 hour. This method produces more MWNTs and few SWNTs[39].

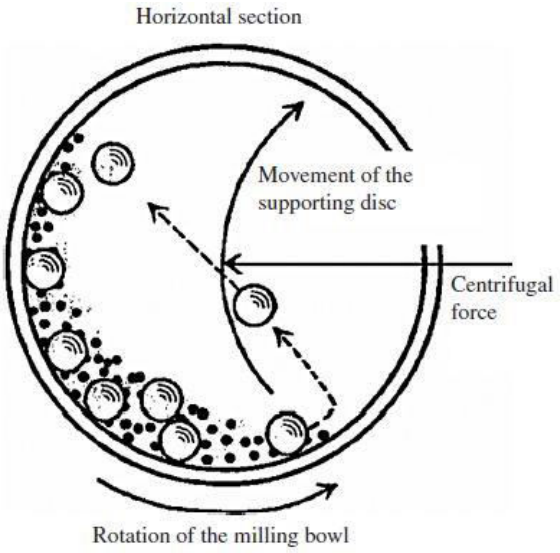

Fig. 1.7: Schematic diagram of ball milling[20]

1.4.4 Chemical Vapor Deposition: From last twenty years, carbon fibers and filaments are produced using chemical vapor deposition of hydrocarbons along with a metal catalyst. In this process, large amount of CNTs is produced by catalytic CVD of acetylene over cobalt and iron. Using the carbon/zeolite catalyst, fullerenes and bundles of SWNTs can be produced along with the MWNTs. Lot of research works have been carried out for the formation of SWNTs/MWNTs from ethylene that is supported by the catalysts such as iron, cobalt, and nickel. The recent research works have also demonstrated the production of SWNTs and DWNTs on molybdenum and molybdenum–iron alloy catalysts. A thin alumina template with or without nickel catalyst is achieved using the CVD of carbon within the pores. Ethylene can be used with reaction temperatures of 545 ºC for Nickelcatalyzed CVD and 900 ºC for an un-catalyzed process that produces carbon nanostructures with open ends. Methane can also be used as carbon source for synthesis. Catalytic decomposition of $H_2$and CH_4mixture over cobalt, nickel, and iron is used to obtain high yields of SWNTs at 1,000 ºC. The usage of H_2 and CH_4 atmosphere between a non-reducible oxide such as Al_2O_3 or $MgAl_2O_4$ and one or more transition metal oxides can produce the composite powders containing well-dispersed CNTs. Thus, higher proportions of SWNTs and lower proportions of MWNTs can be achieved using the decomposition of CH_4 over the freshly formed nanoparticles[40].

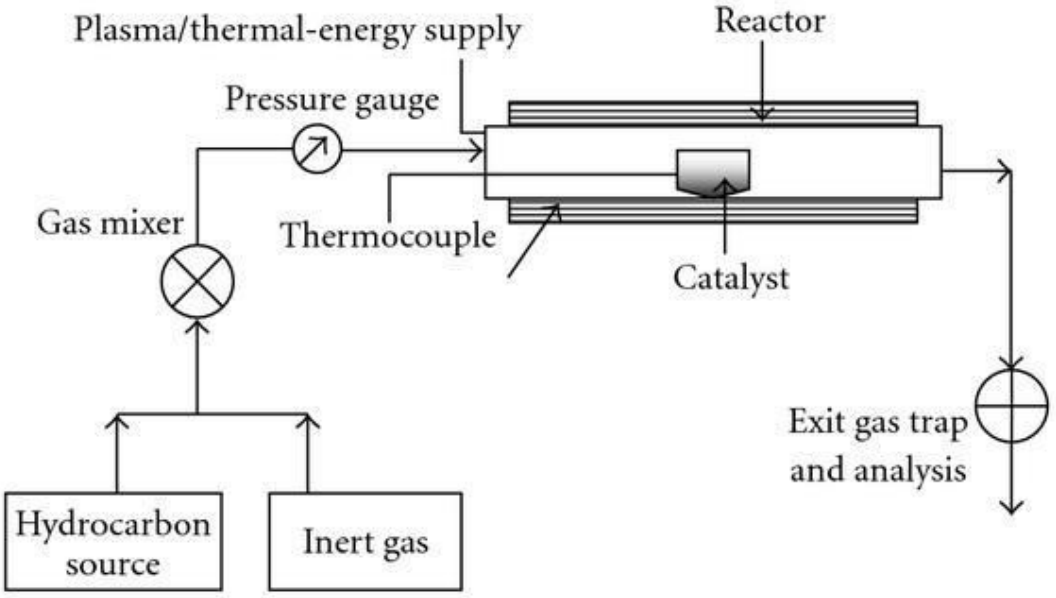

Fig. 1.8: Schematic diagram of Chemical vapor deposition[21]

1.4.5 Other Methods: Apart from the above mentioned synthesis methods, CNTs can also be produced using electrolysis, flame synthesis, synthesis from bulk polymer, use of solar energy and low-temperature solid pyrolysis. Using the electrolysis method, CNTs are produced by passing an electric current in molten ionic salt between graphite electrodes. High purity carbon rod is used as cathode. At high melting point, the cathode is consumed and a wide range of nanomaterials are produced. In the flame synthesis method, a portion of the hydrocarbon gas is provided at an elevated temperature that is required for the hydrocarbon reagents to function. The CNTs can also be synthesized chemically by using polymers consisting of carbon. This process can produce MWNTs with diameters ranging from 5 nm to 20 nm and a length upto1. Several research groups demonstrated the production of fullerenes using highly concentrated sunlight from a solar furnace. Using this method, sunlight is focused on a graphite sample to condense the carbon soot in a cold dark zone of the reactor. The pyrolysis method is used to synthesize CNTs from metastable carbon containing compounds at relatively low temperature of 1200 ℃ to 1900 ℃. This method produces MWNTs of diameters ranging from 10 nm to 25 nm and lengths of 0.1–1μm.

1.5 Applications of Carbon nanotubes[41]:

The applications of CNTs in different fields are listed below:

Structural: CNTs possesses remarkable properties and qualities as structural materials. Their potential applications include:

(a) Textiles—CNTs can produce waterproof and tear-resistant fabrics.

(b) Body armor—CNT fibers are being used as combat jackets. The jackets are used to monitor the condition of the wearer and to provide protection from bullets.

(c) Concrete—CNTs in concrete increases its tensile strength and halt crack propagation.

(d) Polyethylene—CNT fibers can be used as polyethylene. The CNT based polyethylene can increase the elastic modulus of the polymers by 30 %.

(e) Sports equipment—Golf balls, golf clubs, stronger and lighter tennis rackets, bicycle parts, and baseball bats.

(f) Bridges—CNTs may be able to replace steel in suspension and bridges.

(g) Flywheels—The high strength/weight ratios of CNTs enable very high rotational speeds.

(h) Fire protection—Thin layers of buckypaper can potentially protect the object from fire. The dense, compact layer of CNT or carbon fibers in the form of buckypaper can efficiently reflect the heat.

Electromagnetic: CNTs can be fabricated as electrical conductors, semiconductors and insulators. Such applications include:

(a) Bucky paper—Thin nanotube sheets are 250 times stronger and 10 times lighter than steel. They can be used as heat sink for chipboards, backlight for LCD screens, or Faraday cage to protect electrical devices and aero planes.

(b) Light bulb filament—CNTs can be used as alternative to tungsten filaments in incandescent lamps.

(c) Magnets—A strong magnetic field can be generated using multi-walled CNTs coated with magnetite.

(d) Solar cells—Germanium CNT diode exploits the photovoltaic effect. In some solar cells, nanotubes are used to replace the ITO (indium tin-oxide) to allow the light to pass to the active layers and generate photocurrent.

(e) Electromagnetic antenna—CNTs can act as an antenna for radio and other electromagnetic devices due to its durability, light weight and conductive properties.The skin effect in CNTs is negligible at high frequencies due to additional kinetic inductance. This results in low power dissipation, resulting in high antenna efficiency.

Electroacoustic:

The application of CNT in the field of electroacoustic is:

Loudspeaker—Loudspeakers can be manufactured from sheets of parallel CNTs. Such a loudspeaker can generate sound similar to the sound of lightening producing thunder

Chemical:

CNTs finds tremendous applications in the chemical field also, few of them are as follows:

(a) Air pollution filter—CNTs are one of the best materials for air filters because they possess high adsorption capacity and large specific area. The conductance of CNTs changes when polluted gas comes in its contact. This helps in detecting and filtering the polluted air. CNT membranes can successfully filter carbon dioxide from power plant emissions.

(b) Water filter—CNT membranes can aid in filtration. It can reduce distillation costs by 75 %. These tubes are so thin that small particles (like water molecules) can pass through them, while blocking larger particles. CNTs have high active site and controlled distribution of pore size on their surface. This increases not only its sorption capabilities, but also its sorption efficiency. CNTs have effective sorption capacity over broad pH range (particularly for 7 to 10 pH).

(c) Chemical Nanowires—The CNTs finds their applications in nanowire manufacturing using materials such as gold, zinc oxide, gallium arsenide, etc. The gold based CNT nanowires are very selective and sensitive to hydrogen sulphide (H_2S) detection. The zinc oxide (ZnO) based CNT nanowires can be used in applications for light emitting devices and harvesters of vibrational energy.

(d) Sensors—CNT based sensors can detect temperature, air pressure, chemical gases (such as carbon monoxide, ammonia), molecular pressure, strain, etc. The operation of a CNT based sensor is primarily dependent on the generation of current/voltage. The electric current

is generated by the flow of free charged carrier induced in any material. This charge is typically modulated by the adsorption of a target on the CNT surface.

Mechanical: The potential application of CNTs can be found in the following areas of mechanical engineering as well:

(a) Oscillator—Oscillators based on CNTs have achieved higher speeds than other technologies (>50 GHz). Researchers reported a molecular oscillator with frequencies upto several gigahertz. The operation of this oscillator is primarily based on the low friction and low wear bearing properties of a multi-walled CNT with a diameter ranging from 1 nm to a few tens of nanometers.

(b) Waterproof—CNTs can be used to prepare super hydrophobic cotton fabric by dip-coating approach. This approach is solely based on the chemical reactions caused by UV-activated nitrene solution. The solution is used to transform the cotton fabric surface from hydrophilic to super hydrophobic with an apparent water contact angle of 154º. Since CNTs are covalently attached on the surface of the cotton fabric, the super hydrophobicity possesses high stability and chemical durability.

Optical: Carbon nanotubes are grown like a field of grass, where each nanotube is separated like a blade of grass. Thus, a particle of light bounces between the nanotubes. In this process, light is completely absorbed and it is converted to heat. Therefore, the absorbance of CNT is extremely high in wide ranges from FUV to FIR[FUV (Far Ultraviolet): 100-200 nm; FIR (Far Infrared): 50-1000 µm].

Electrical Circuits: CNTs are attractive materials in fundamental science and technology. They have demonstrated unique electrical properties for building electronic devices, such as CNT field-effect transistors (CNTFETs) and CNT diodes. CNTs can be used to form a p–n junction diode by chemical doping and polymer coating. These types of diodes can be used to form a computer chip. CNT diodes can potentially dissipate heat out of the computer chips due to their unique thermal transmission properties.

Interconnects:

Carbon nanotubes (CNTs) have emerged as one of the most potential interconnect material solutions in current nanoscale regime. The higher current density of 1000 MA/sq-cm of an isolated CNT can eliminate the electron migration reliability concerns that plagues the current

nanoscale copper interconnects. Therefore, CNT interconnects can potentially offer immense advantages over copper in terms of crosstalk, delay and power dissipation.

Transistors: CNTs can form conducting channels in transistor configurations. Two different device architectures have been developed for the transistor configuration. In both cases, CNTs connect the source and drain electrodes and show excellence behavior in the area of memory designing, amplifiers, sensors and detectors, etc. In one device architecture, the source and the drain are connected by a single nanotube. In other device architecture, a random array of nanotubes functions as a conducting channel .The advantages of CNTFET over Si-MOSFET are as follows:

(i) CNTFET demonstrates higher drive current compared to Si-MOSFET.

(ii) CNTFET shows approximately four times higher transconductance than Si-MOSFET.

(iii) The average carrier velocity of CNTFET is almost double the Si-MOSFET. This chapter presented the unique atomic structures, properties and applications of carbon nanotubes. The electrical, mechanical and thermal properties of CNTs are primarily dependent on their diameter and chirality. In addition to this, the chapter summarized different production and purification methods for SWNTs and MWNTs.

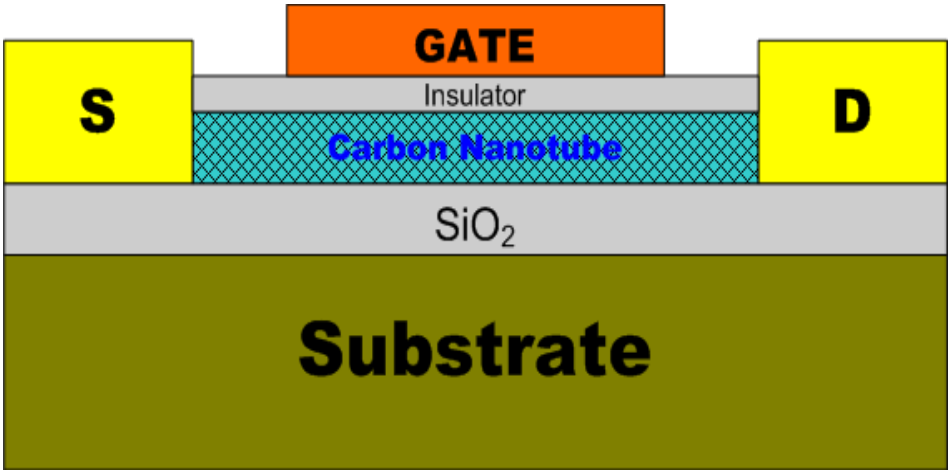

Fig. 1.9: Application of carbon nanotube with transistor

1.6 Filling of Carbon nanotubes :

1.6.1 Filled and Un-filled multi wall carbon nanotubes: Basically the methods for the synthesis of un-filled and filled carbon nanotubes are similar. At both processes hydrocarbon precursor compounds are required which deliver the carbon for the formation of the CNT-walls. Additional, since it is a catalytic process, a catalyst (in this case a metal) is involved to control the kinetics of reactions such as the decomposition of the precursor. It also acts as a geometric confinement for the forming CNT-structure. The catalyst can be located on a substrate or is delivered via the gas phase. The latter is often called a floating catalyst process. While for empty CNT beside the metal-organic compound an additional hydrocarbon (mostly liquid or gaseous) is very often used, the deposition of highly filled carbon nanotubes is realized by only metal-organic compounds. Because these compounds also possess a convenient temperature range for sublimation and thermal decomposition, the metallocenes are the usually used precursors for filled carbon nanotube synthesis. Especially the metallocenes, ferrocene, cobaltocene and nickelocene contain the transition metals Fe, Co and Ni respectively. It is well known these metals have a low carbon solubility, form only metastable carbides and are so able to act as efficient catalyst.

By using only such metallocenes the filling and the forming of the carbon nanotube is a simultaneous process (the so-called in-situ filling process). Other strategies, e.g., for an ex-situ filling of nanotubes in a separate step after the growth of empty, hollow CNT are not reconsidered within this review and are reported elsewherewe focus on the in-situ filling processes[42].

Metallocenes: A metallocene is typically a compound comprising of two cyclopentadienyl anions (Cp, that is $C_5H_5^-$) bound to the metal center (M) in oxidation state II, alongwith the resulting general formula being $(C_5H_5)2M$. Very closely related to metallocenes are the metallocene derivatives, for example, vanadocene dichloride, titanocene dichloride. Some metallocenes and their derivatives are found to exhibit catalytic properties, even though metallocenes are very rarely used industrially. The cationic group 4 metallocene derivatives are related to the $[Cp_2ZrCH_3]^+$catalyze olefin polymerization. The metallocenes are the subset of a broader class of the organometallic compounds that are termed as the sandwich compounds.

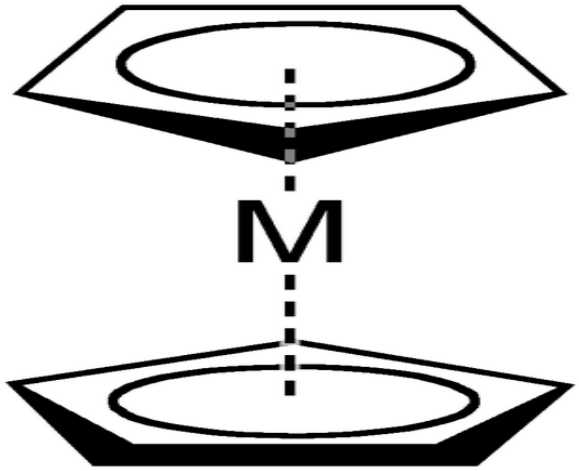

Fig. 1.10:Representation of metallocene[12]

The first metallocene that was be classified was the ferrocene, and it was discovered simultaneously by Keally and Pauson and also, Miller in 1951. Keally and Pauson attempted to synthesize fulvalene by the oxidation of cyclopentadienyl salt with the anhydrated FeCl3 but instead, they obtained the substance $C_{10}H_{10}F$. At the same time, it was reported that Miller synthesized the same iron product through a reaction of cyclopentadiene with the iron in presence of potassium, aluminum, or molybdenum oxides. Wilkinson as well as Fischer determined the structure of the "$C_{10}H_{10}Fe$" and they were awarded the Nobel Prize in 1973 in Chemistry for their great work on sandwich compounds, which included structural determination of ferrocene. It was they who determined that carbon atoms of cyclopentadienyl (Cp) ligand strongly contributed equally to bonding and this bonding occurred because of the metal d-orbitals and also, the π-electrons in p-orbitals of those Cp ligands.This complex is now termed as ferrocene and this group of transition metaldicyclopentadienyl compounds is termed as metallocenes and they have the general formula [(η5-C_5H_5)2M].Fischer prepared the ferrocene derivatives involving Co and Ni first amongst all. Most often derived from the substituted derivatives of cyclopentadienide, the metallocenes of many such elements have been prepared.

Definition: General name “metallocene” is derived from the term “ferrocene”, Cp_2Fe or $(C_5H_5)_2Fe$, named systematically bis(η5-cyclopentadienyl)iron(II). According to IUPAC definition, any metallocene contains a transition metal alongwith two cyclopentadienyl ligandsthat are coordinated in a sandwich structure, i. e., these two cyclopentadienyl anions are on the parallel planes with equal bond strengths and lengths.With the use of the

nomenclature of "hapticity", equivalent bonding of all these 5 carbon atoms of cyclopentadienyl ring is termed as η5, and pronounced "pentahapto".

1.6.2 Properties of filled CNTs:

Magnetic Properties: Typical hysteresis loops were measured for the filled carbon nanotube carpet on the pre-coated silicon substrate. The measurements always reveal a uniaxial magnetic anisotropy with the easy axis along the tube axis. Saturation magnetization M-sat and coercivity HC are dependent not only on the ferromagnetic bcc-iron fraction, but also on the alignment level, and diameter and length of the filled carbon nanotubes on the substrate. For example, the higher the growth rates, the stronger is the alignment; magnetic anisotropy also increases with increasing lengths. This means the aspect ratio determines the magnetic anisotropy (so-called shape anisotropy). Moreover, it should be noted that values of coercivity reached are far higher than for the bulk material (max. HC(Fe) in Fe-filled tube carpets = 130mT, compared to bulk HC(Fe) = 0.009 mT). With an increase in the growth temperature the diameter of the encapsulated Fe nanowires becomes larger. This effect decreases the coercivity, the magnetic hardness, and hence, reduces the magnetic anisotropy. As shown here, dependence on the parameters of the growth process can strongly affect the magnetic properties. The most important variables are the growth temperature and the sublimation temperature of ferrocene, because these parameters strongly affect the diameters, lengths, and alignment of the nanotubes[43].

Electronic Properties: CNTs have been found to be very good field emitters with low turn – on fields and high current densities. This has made them attractive as possible electron sources in, for instance, electron microscopes and cathode ray oscilloscopes. It has been found that arrays of CNTs filled with iron oxide has a lower turn-on field than unfilled CNTs. Numerous studies have been conducted till date on the field emission from standard unfilled CNTs that have linked the field emission properties of the CNTs to their structural properties. However, there is very little data available on the field emission properties of filled CNTs, particularly individual filled CNTs[43].

1.6.3 Applications of filled CNTs:

The structures of the nanotubes may be imagined as metal nanomagnets or nanowires within the carbon nanotubes. These nanowires are strongly protected by encapsulation against the oxidation and most other chemical reactions and influences. Thus, such nanowires exhibit long-term stability. Hence, this is a magnanimous advantage compared to uncoated, pure nanowires, and thus, opens new application fields.

These ferromagnetic-filled carbon nanotubes find applications ranging from the magnetic data-storage devices, to the implementation of individual filled tubes in any sensor system for the magnetic force microscopy.

Another probable utility of filled carbon nanotubes is observed in the field of biomedicine as ferromagnetic nanocontainers initiating a novel anti-tumor therapeutic concept in treatment of the cancer disease. Furthermore, exceptional electronic properties and hollow structure characteristic of these CNTs could have a significant potential for the use of these magnetic nanotubes in many other applications which ranges from electromagnetic devices to the magnetically guided drug delivery system. The filled carbon nanotubes represent a befitting material for the magnetically guided hyperthermia and, also, functionalized inside and outside the tube, a very unique drug delivery/carrier system.

1.6.4 Growth mechanism of filled CNTs:

Analyzing the growth mechanisms of the carbon nanotubes is a prime requisite for the desired synthesis to obtain certain special properties that are needed for the desired applications. Up to now there is no generally accepted growth mechanism and further research is necessary. The knowledge and understanding of the mechanism is under continuing development and several modifications were discussed during the last two decades. A few widely discussed mechanisms are mentioned below:

VLS mechanism: The basis of all is the vapor-liquid-solid (VLS) mechanism which was originally developed for the growth of silicon whiskers by Wagner and Ellis. It consists of the assumption that a gaseous phase, a liquid phase and a solid interacts. The precursor is supplied as the gas. The liquid phase is liquefied molten catalyst particle present on the solid substrate. During this growth process it is observed that the precursor decomposed in a specific area of the surface of the liquid particle at the temperature T_1. The precursor material

dissolves until saturation at concentration c_1 is attained. It is assumed that this particle occupies an area with a lower temperature T_2 and a lower concentration c_2. Thus the presence of both a concentration and thermal gradient is assumed. Precursor materials diffuse through the particle and precipitates at T_2. These very basic assumptions of the mechanism allow the application to other systems.

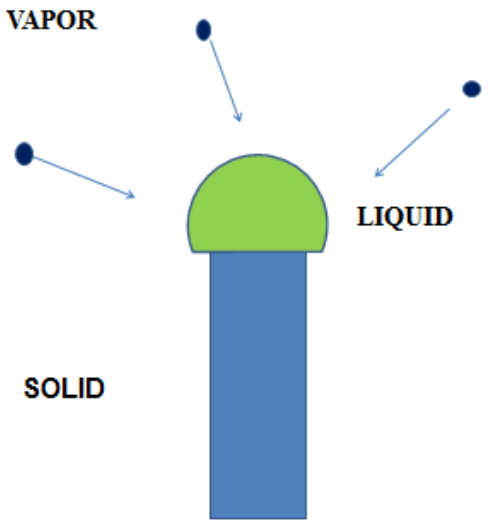

Fig. 1.11: VLS growth mechanisms[13]

Base and tip growth mode:

This is one of the very first mechanism to explain growth of the carbon whiskers which was initially developed by Baker on basis of VLS mechanism. He and his group performed in-situ studies on growth of the carbon whiskers by employing controlled atmosphere electron microscopy (CAEM). During this formation, the liquefied metal catalyst particles were either on tip or bottom of as-formed whiskers. Because of the forces acting on these catalyst particles, they undergo deformation during the process which results in two different growth modes. If thereis strong attractive interaction between catalyst and substrate, then a good wettability is found which lead to the contact angles below 90˚ and these particles are found to be most likely remains on the surface of substrate. Since decomposition of the hydrocarbons relies on catalytic activity of the particle surface which supplies carbon atoms can solely connect to already existing carbon structures present at the particle whisker interface. Thus, the oldest part of whisker is the tip while the youngest part is the bottom. This is why it is termed as the base growth mode. On the other hand, if there is a repulsive

interaction between particle and surface then, a contact angle more than 90˚ will be established. The particle then most likely detaches itself from the surface and lifts itself up. In this case, thus, the oldest part of CNT is nearest to the substrate surface while the youngest part is tip. Thus, this is termed as the tip growth mode.

In the figure: 1(k), it is showed that the metal particles on the surface are exposed to gaseous hydrocarbons, which decompose catalytically on the surface of the catalyst particle. An exothermic decomposition is assumed and a carbon concentration as well as a temperature gradient form. After its decomposition the carbon diffuses from the hot area with a higher concentration to the colder region of the particle and precipitates to form the graphitic structure of the CNT wall. The particle remains attached to the substrate

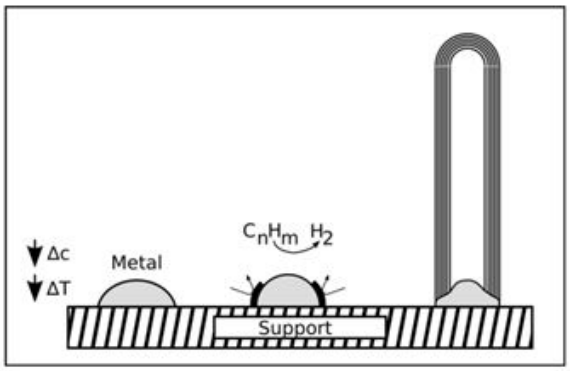

Fig. 1.12: Base growth[14]

In the figure1(l), it is showed that the metal particle is only weakly bound to the substrate surface. The decomposition of the hydrocarbons takes place at the upper side of the particle. Again an exothermic decomposition is assumed and the temperature and carbon concentration increases at the top of the particle which gets deformed during this process and detaches from the substrate. The carbon now diffuses to the colder side of the particle and precipitates to form the CNT shells.

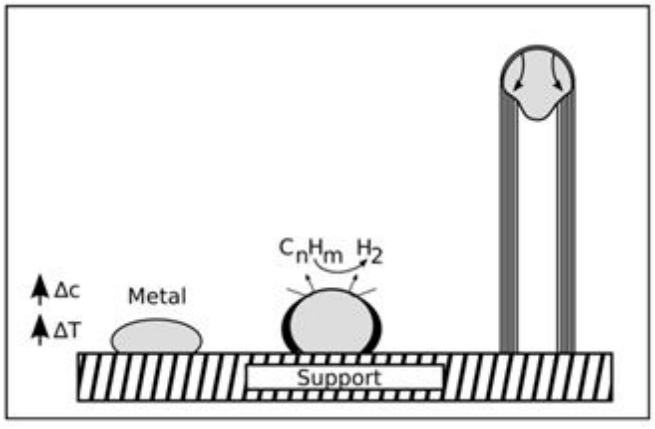

Fig. 1.13: Tip growth[15]

Base and tip growth mode for filled CNT

For filled CNT, not only the formation of the carbon shells but also the formation of the in-situ filling has to be explained. However, it is specifically difficult to describe the influence of the catalyst because it is applied on the substrate and additionally as floating catalyst from the decomposed precursor. During the whole growth process metal particles, mostly catalytically active, do interact with the forming CNT. Nevertheless, several groups adjusted the VLS mechanism and the concepts of the tip and base growth mode to explain the formation of in-situ filled CNT. From the experiments carried out by Zhang indicated a growth mechanism that could easily explain the in-situ filling of carbon nanotubes with iron during synthesis. This scheme of the mechanism is thus shown in Figure 1(n). The figure presents the growth process of in-situ filled CNT. (A) shows the slow growth stage. The carbon shells at the open tip react with carbon clusters from the gas phase. In (B) a larger catalyst particle attaches to the open tip and the fast growth stage starts. The CNT grows fast and the pressure caused by the shells deforms the catalyst particle. In this stage (C) a filling section is formed. If the supply with catalyst material stops the slow growth stage continues[44].

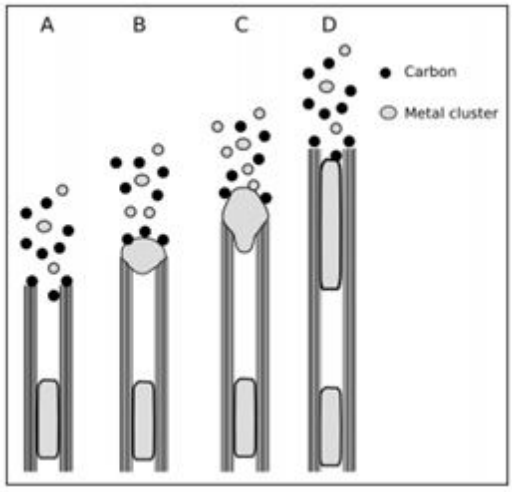

Fig. 1.14: Base and tip growth mode for filled Carbon nanotube[16]

Combined growth mode:

An intensive discussion and interesting approach to explain the growth of metal-filled CNT was presented by Kunadian. They combined tip- growth and base-growth mode explaining the formation of the filling in the context of a closed tip growth process. In the

continuous-feed CVD the precursor containing both the carbon source and the catalyst material is provided continuously during the process. In the mechanism it is assumed that the initial state follows the base growth mode. Hydrocarbons decompose on the surface of these catalyst particles. Because of the floating catalyst conditions metal clusters are formed and hydrocarbons can also decompose already in the gas phase. The catalytically active metal clusters and the carbon atoms fall onto the catalyst particles which remain anchored to the surface of substrate. It may be assumed that this results in a continuing change in catalyst conditions. Each and every cluster that connects to catalyst particle modifies the volume, shape and the carbon concentration of the catalyst. Thus under these floating catalyst conditions it is very likely that the growth mode switches from the base to tip growth mode. After the switching takes place, the filling process and also, the shell formation occurs simultaneously at the tip.

Figure gives the steps of the combined growth mechanism. In step (A) a catalyst particle is formed. Step B describes the decomposition of hydrocarbons on the particle surface. Due to the floating catalyst method catalytic processes occur also in the gas phase forming metal and carbon clusters. In step C the deposition of iron particles at the growing site takes place continuously,thereby the growth mode changes from base to tip growth mode (step C-D). When further material deposits from the gas phase the growth continues (step E) until a stable cap is formed. If the cap is closed so called secondary growth might occur. This is often tip growth since the wettability of the metal catalyst is low and the particles easily detach (step F and G)[44].

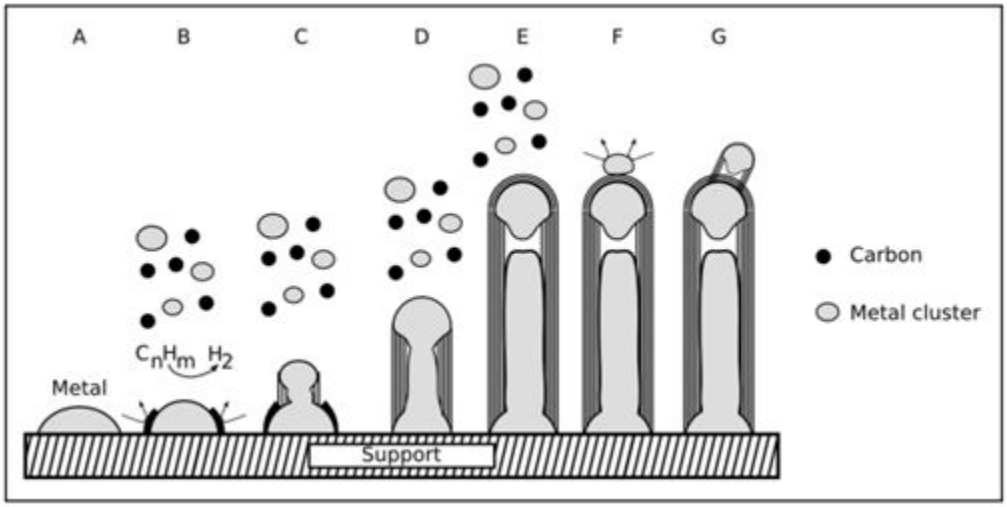

Fig. 1.15: Combined growth mode[17]

Chapter 2 Literature survey

A literature survey forms an important and indispensable module of a research project. It throws light on the amount of study done so far in the chosen subject matter, showcases the flaws and gaps in the previous research, pinpoints the new scopes of research arising out of those studies ,highlights the status of research being carried out by the contemporary research groups in the relevant field around the globe and finally ,saves time, funds and energy of a researcher from ending up in some conclusions which have already been found out by some other research group at some early date. Also, it prevents the research knowledge base from being plagued by plagiarism to a great extent.

A substantial amount of literature review has been done in this project. This provides a summary on the different synthesis methods for the thermo gravimetric analysis of filled CNTs, adopted by different research groups and their pros and cons as well as their feasibility in commercialization. Moreover,it throws light on the study carried out around the globe on the properties and ways and means to tailor them as per the needs of the industry.

Some studied papers are as follows:

1. Pawan K. Tyagi et al.[1] reported that Carbon nanotubes (CNTs) filled withferromagnetic materials have the potentials for use in magnetic scanning probe microscopy and as an assembly of aligned high density magnetic nanocores for future magnetic data storage devices. Highly ordered and uniform Ni-filled CNTs were deposited by chemical vapour deposition. As-grown Ni-filled CNTs were characterized using transmission electron microscopy, Raman spectroscopy and nano-area diffraction. The magnetic properties of Ni-filled CNTs were investigated a using superconducting quantum interference device analysis.Magnetizationcharacterization, performed at temperature 2 K with magnetic field up to 2 T, showed better ferromagnetism compared to the bulk Ni.
2. Reetu Kumari et al [2] reported that present study aims to deduce the confinement effect on the magnetic properties of iron carbide (Fe_3C) nanorod filled inside carbon nanotube (CNT) and to document any structural phase transitions that can be induced by compressive/tensile stress generated within the nanorod. Enhancement in the magnetic properties of nanorods is attributed to tensile stress

as well as compression present in radial direction and along the nanotube axis, respectively. Finally, growth of permanent cylindrical nanomagnets has been optimized by applying field gradient. Besides presenting the growth model of in situ filling we have also proposed the mechanism of magnetization of the nanotubes. Magnetization along the tube axis has been probed by confirming the pole formation. Fe_3C has been selected because of easy formation, low TC and incompressibility.

3. Lucky Krishnia et al.[3]described that filled or un-filled multiwalled carbon nanotubes (CNTs) used in this study have been synthesized by the floating catalyst method and fixed catalyst method, respectively. The thermal stability of filled/un-filled carbon nanotubes has been investigated by using Thermogravimetric analysis (TGA) and Derivative thermogravimetric (DTG) analysis. In this report, we have developed a methodology to distinguish between filled and un-filled carbon nanotubes. Filled-CNTs are found to be more resistant to oxidation than the un-filled carbon nanotubes. The calculated activation energy of as-grown filled CNTs, by using differential method, determined to be 3.29 ± 0.04 eV, which is higher than that of highly ordered pyrolytic graphite (HOPG). Carboneous impurities; amorphous carbon, catalyst and CNT of different diameter, which are structurally different, are identified by their reactivity and the resistance to oxidation.
4. Lucky krishnia et al.[4] reported in this article that thermal stability and reactivity of oxygen to Fe_3C-filled and un-filled multi-walled carbon nanotubes (MWCNTs) have been studied by using thermogravimetric analysis (TGA) and derivative thermogravimetric (DTG) analysis. Exclusively, oxidation of sample containing Fe_3C-filled MWCNTs is found to be endothermic upto 600 °C. The value of activation energy of oxidation is determined by fitting the experimentally recorded TGA/DTG curves, and both differential and integral methods have been adopted for calculation. The calculated value of activation energy for Fe_3C-filled MWCNT using Kissinger's corrected kinetic equation (integral method) is found to be 1.48 ± 0.19 eV, which is nearly equal to the reported values for highly ordered pyrolytic graphite (HOPG). Oxidation reactivity is found to follow an ascending order as amorphous carbon, thin MWCNTs, un-filled MWCNTs, and Fe_3C-filled MWCNTs.

5. G. Che et al.[5] have developed a novel approach for the preparation of graphitic carbon nanotube and nanofiber ensembles. This approach comprises of chemical vapor deposition (CVD) based synthesis of carbon inside the pores of an alumina based template membrane with or without Ni catalyst. Pyrene or ethylene was used in this CVD process with furnace temperatures of about 545 °C for Ni-catalyzed CVD while 900 °C for the uncatalyzed one. The as-synthesized carbon nanostructures were uniform hollow tubes having open ends. On increasing the deposition time the carbon nanotubes gets converted into carbon nanofibers. Electron diffraction data and transmission electron microscopy show the as-deposited graphitic carbon nanofibers that were synthesized with Ni catalyst were found to be not highly ordered. However, heating these carbon-containing membranes at 500 °C for 36 h, converts these carbon nanofibers into highly ordered graphite.
6. Rajashree Hirlekar et al.[6] reviewed the existing literature on CNTs around the globe. They have summarized the history of Carbon nanotubes (CNTs), right from the chemical composition and physical dimensions to the novel properties that make them potentially way better traditional devices in the relevant fields. The techniques developed for their production of nanotubes in sizeable quantities, are listed by them. The properties and characteristics of CNTs are still to be exploited. They reported that the promising properties of CNTs can bring a revolution in the field of medicines.
7. Uhland Weissker et al.[7] presented an overview about different available chemical vapor deposition (CVD) methods for the synthesis of CNT filled with different ferromagnetic materials such as iron, cobalt or nickel, in addition to the influence of the various growth parameters. Besides that, they evaluated the possible growth mechanisms which are involved in the 30 formation of CNTs. Moreover, they studied their structural and magnetic properties based on which their different application possibilities were presented.
8. A. Leonhardt et al.[8]reported Single- and multi-walled carbon nanotubes are very interesting nanoscaled materials with many possible applications in nanoelectronics. Especially, nanotubes filled with ferromagnetic materials (Fe, Co, Ni) may have significant potential in data storage. Such structures may help to exceed the best available storage densities (>65 Gb/inch^2) and show in the case of Fe-filled nanotubes higher coercivities compared to bulk Fe. In addition, metal-

filled carbon nanotubes are promising nanowires with excellent oxidation protection. In this paper we describe the synthesis of Fe-, Ni- and Co-filled carbon nanotubes by using the chemical vapor deposition method. Varying the deposition conditions we have obtained filled nanotubes with relatively uniform core diameters and different thicknesses of the carbon walls. The core diameters vary between 15 and 30 nm and the thickness of the carbon shells between 2 and 60 nm. The length of the tubes amounts up to 30 μm. The filled carbon nanotubes are characterised by scanning and transmission electron microscopy and energy dispersive X-ray analysis. The magnetic behaviour of the aligned Fe-filled tubes is investigated using alternating gradient magnetometry measurements and electron holography. The hysteresis loops indicate a magnetic anisotropy. The coercivity depends on the direction of the applied magnetic field. The observed enhanced coercivities are significantly higher than in bulk Fe.

9. Martin Moskovits et al.[9]provides a powerful new method for producing, uniform sized and uniformly aligned nanotubes through catalytic pyrolysis of a hydrocarbon within the dense, uniform and parallel pores of alumina nano-templates. The catalyst, Co, Fe, Ni or another suitable substance is deposited electrochemically into the bottom of the channel of the alumina template. The nanotubes with any desired diameter in the range 5-500 nm and lengths up to ˜100 μm, are generated by the pyrolysis of a suitable hydrocarbon inside the pores of the alumina template with at least one end open at the alumina/air interface. The nanotubes may be filled by metals using for example electron less deposition.
10. Guzeliya et al.[10] describe a simple and versatile technique to produce magnetic tubes by filling carbon nanotubes (CNTs) with paramagnetic iron oxide particles (∼10 nm diameter). Commercial ferrofluids were used to fill CNTs with an average outer diameter of 300 nm made via chemical vapor deposition into alumina membranes. Transmission electron microscopy study shows a high density of particles inside the CNT. Experiments using external magnetic fields demonstrate that almost 100% of the nanotubes become magnetic and can be easily manipulated in magnetic field. These one-dimensional magnetic nanostructures can find numerous applications in nanotechnology, memory devices, optical transducers for wearable electronics, and in medicine.

Chapter 3 Experimental procedure

In this chapter we will discuss all the experiments carried out throughout the span of project work, their set ups, yield, methodology and how we came up with the optimized procedure. All the experimental work was carried out in the Nano fabrication lab, Department of Applied physics at DTU.

3.1 Synthesis technique adopted: Thermal CVD –Thermal CVD is a robust method for the growth of high-quality carbon nanotubes that ranges from the single-walled to the multi-walled to the metal-encapsulated carbon nanotubes. This method is fit to produce a large quantity with satisfactory quality and also, allows upscaling at some moderate costs for the industrial mass production. Under the ideal conditions, thermal CVD growth forms the primarily individual tubes instead of tubes in bundles. Also, the process can be tailored in order to promote either the single- or the multi-walled (MW) carbon nanotubes growth. This in situ filling of CNTs using thermal CVD with nickel finds application in the magnetic scanning probe microscopy as well as the assembly of aligned high density magnetic nanocores for future magnetic data storage devices. A real time lab set up for Thermal CVD is given below:

Fig. 3.1: Picture of CVD furnace at Delhi Technological University

3.2 Apparatus and Precursors used:

In order to complete the entire set up of experiment a number of apparatus and precursors are needed, here in this topic we will name and if necessary, explain each one of them.

1. **Silicone pipe**: To transport the precursors inside the tube to carry out the reactions it is needed. The length of used pipe in our experiment is 1 m with an internal diameter of 38 mm and external diameter of 40 mm.

2. **Ultrasonicator**: As in this experiment a solution of metallocene with the hydrocarbon is required so to make such solution ultrasonication is performed.

3. **Thermal CVD furnace**: This requirement is shown in the above section.

4. **Quartz tube**: This tube goes inside the furnace and in the hot zone of this tube the reactions are carried out.

5. **Hydrogen and Argon gas cylinders**

6. **Mass flow controller**

7. **Syringe Pump**

Precursors:

(i) Nikelocene: The Nickelocene is organonickel compound having the formula Ni(η5-C5H5)2. It is also termed as bis(cyclopentadienyl)nickel or NiCp2. It is a bright green paramagnetic solid and is of persisting academic interest, even although it has yet no practical applications.It provides for the encapsulated Ni inside the synthesized CNTs.

Structure and Bonding:

$Ni(C_5H_5)_2$ belongs to the group of the organometallic compounds known as the metallocenes. These metallocenes usually adopt structures wherein a metal ion is found to be sandwiched between the two parallel cyclopentadienyl (Cp) rings. The structure is quite relevant to the solubility in the organic solvents and also, volatility. In solid-state, this molecule has the D5h symmetry, in which the two rings are eclipsed.

Ni center has the formal 2+ charge, while, Cp rings are assigned usually as the cyclopentadienyl anions (Cp−), that are related to the cyclopentadiene by the deprotonation. The structure is thus, similar to the ferrocene. In the terms of its electronic structure, the three pairs of d electrons on the nickel are allocated to three d orbitals that are involved in the Ni - Cp bonding: dxy, $dx_2–y_2$, dz_2.Out of the remaining two, one d-electrons is placed in each of dyz and dxz orbitals, that gives rise to this molecule's paramagnetism, as observed in the exceptionally high field chemical shift that is observed in its HNMR spectrum. With some 20 valence electrons, the nickelocene has the highest electron count, out of the transition metal metallocenes.

(ii) Benzene: It has a two-fold role in the experimental process – firstly, being the provider of carbon for CNT preparation and secondly, as a solvent for Nickelocene.

3.3 Optimization of SynthesisParameters: The entire experiment is optimized in order to get better yield according to three parameters namely, temperature, concentration of Nickelocene and gas flow.

1. **Temperature**: The synthesis of Ni filled CNTs are carried out on various temperature as the production of CNTs starts at 700 °C but the yield is very low so in order to get a better yield the temperature of the furnace is varied and in the beginning of the experiments it was kept around 850 °C which then reduced to 820 °C in order to get a better yield.
2. **Concentration of Nickelocene**: It is very crucial to keep an adequate amount of Nickelocene as it provides for the encapsulated metal and if kept low only hollow CNTs are going to be synthesized. And if kept high encapsulation might not even take place.
3. **Gas flow rate**:It is another very important factor which plays a crucial role in the formation of filled CNTs and during the course of our experiment it has been varied to get the best possible result.

3.4 Experimental condition:

Upon going through a lot of literatures i decided to start the work but until now I was not decided upon the solvent because there were a number of non-polar solvents like Toulene, Benzene, Di chlorobenzene, THF etc. but solubility of nickelocene was still a

concern and in order to make a solution, I decided to sonicate the solvent(Benzene)and the solute(Nickelocene).

Any Non polar solvent will solve the purpose but I decided to use Benzene because of its ready availability and less toxicity in comparison to Xylene.

Steps in experiment:

1. Cleaning of quartz tube.

2. Making the solution of Nickelocene and Benzene.

3. Setting up the furnace with protection and precaution.

4. Obtaining the synthesized sample.

5. Removal ofNon-magnetic impurity from sample.

Flow chart:

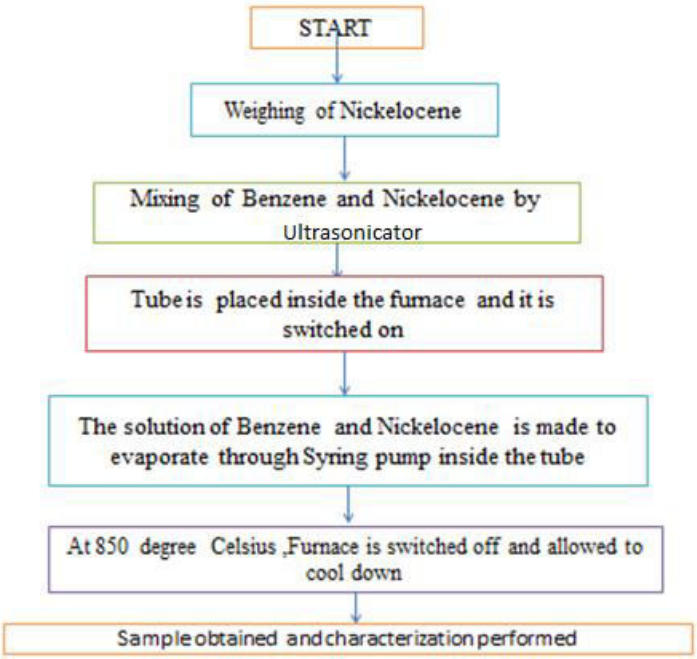

Fig. 3.2: Flow chart of entire experimental process

Flow Diagram :

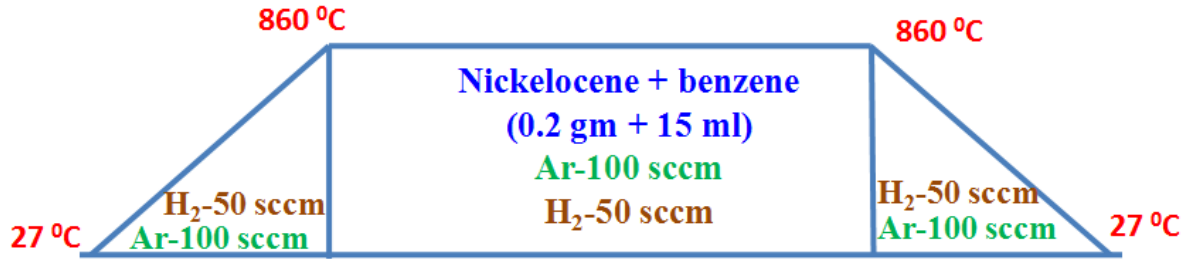

Fig. 3.3: Schematic of experimental conditions

The above diagram is an approximate flow for the entire furnace process. Here, it is simply a generic one in order to understand the technique but later in our experimental trials, we will see that process might be altered in order to optimize the yield.

Here it is being shown that the entire process will start at a room temperature and goes linearly up to a desired temperature (850 °C in this case) with the solution of the precursors inside the tube as well as with required gas flow of hydrogen and argon. Some what this is the process which I followed throughout all the experiment barring a few. Now, I will give the experimental details one by one for every experiment.

Schematic Diagram:

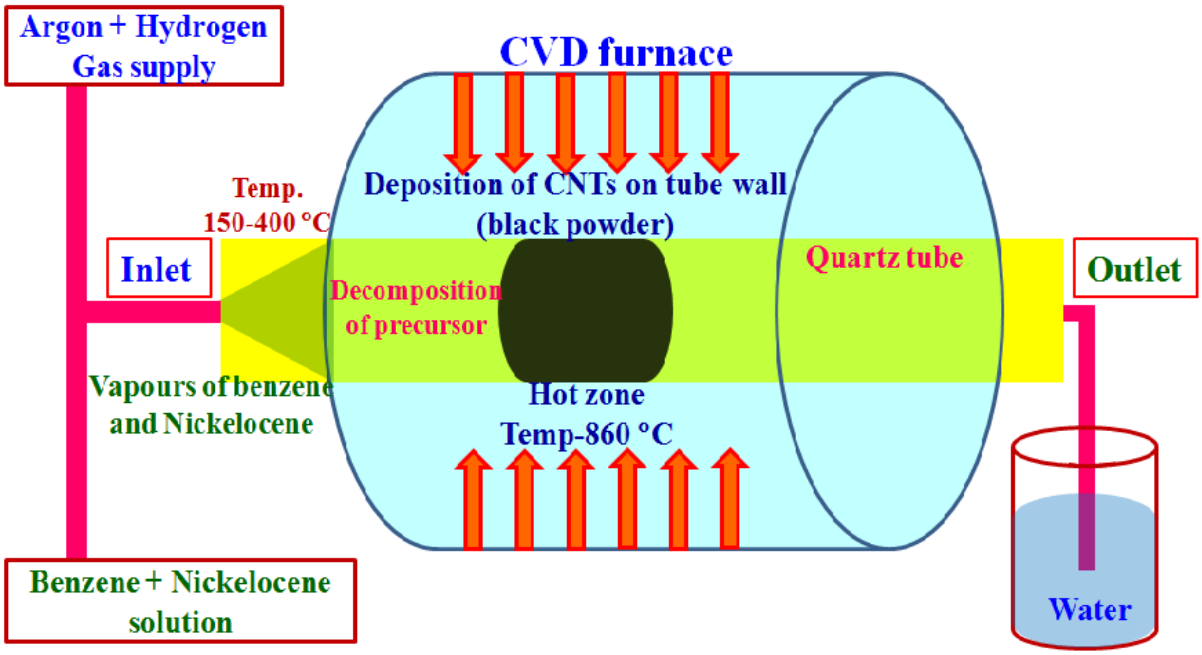

Fig. 3.4: Experimental setup for synthesis of Ni filled CNT using CVD furnace

Trial No.1:

a) Cleaning of quartz tube: The tube is a cylindrical tube which has heat handling capacity better than glass and as the technique used here is Thermal CVD, it is bound to be in the range of 500 to 1000° C. The tube is being cleaned using hydrochloric acid with a concentrated measure so proper precaution like rubber gloves, apron should be taken and wore. I cleaned the tube thoroughly twice and let it dry and again the next day it has been cleaned with the use of acetone for left over impurities and again left to evaporate.

b) Making solution of Nickelocene and benzene: The solution is made by the use of ultrasonication process where the solute and the solvent are kept in the sonicator and shaked at a very high frequency in order to mix them properly. Sonication is a method in which sound waves are used to agitate particles in the solution. Such disturbances can be used to mix solutions, speed the dissolution of a solid into a liquid and can be remove dissolved gas from liquids in some cases too.

In the very first trial I took 20 ml of Benzene and mixed 0.2 gm of Nickelocene in it and sonicated it for 10 min, the obtained solution was a not a true solution but there were no suspension visible to naked eye as well as there were no sedimentation. Once the solution was prepared it as kept in the bottle with the nozzle and start preparing the furnace.

c) Setting up Furnace: The thermal CVD furnace in the laboratory is checked and the quartz tube is inserted into it, on the one side the quartz tube is attached with the silicone pipe to the syringe pump with flow rate of 0.35 ml/min containing solution and to the gas cylinder through gas regulator which regulates the flow rate as well as displays the rate. The other side of the tube is connected to the thermocouple for getting time to time exact temperature of the tube inside and also this side is being used to release the waste fume out of the tube. Once the furnace set up is done we start the furnace with room temperature take it up to 750 °C and once this temperature is reached the solution is made to evaporate inside the tube and once all the solution is evaporated we started cooling down the furnace back to room temperature.

d) Collection of sample:The next day of the experiment the cooled quartz tube is taken out of the furnace and the deposited black powder/ flake on the wall of the tube is

scratched with the help of a brush and a rod. The obtained sample is carefully taken into a vial and kept for characterization.

e) Result: Very small amount of black powder collected and after characterization, No CNT like structure formed.

Amount of Precursor	Gas used	Flow rate	Temperature
20ml Benzene 0.2gmNickelocene	Hydrogen Argon	50 100	25 to 750°C

Table: 3.1 Specifications relating to Trial no. 1

Trial No.2:

We changed the temperature from 750 to 775° c and syringe pump flow rate from 0.35ml/min to 0.3ml/min and kept all other conditions same.

Amount of Precursor	Gas used	Flow rate	Temperature
20ml Benzene 0.2gmNickelocene	Hydrogen Argon	50 100	25 to 775°C

Table: 3.2 Specifications relating to Trial no. 2

Result: Sample obtained like crispy flakes and after characterization CNT like structure is not obtained.

Trial No. 3:

We changed the temperature from 775 to 800° c and kept all other conditions same.

Amount of Precursor	Gas used	Flow rate	Temperature
20ml Benzene 0.2gmNickelocene	Hydrogen Argon	50 100	25 to 800°C

Table: 3.3 Specifications relating to Trial no. 3

Result: Sample obtained like black powder and after characterization CNT like structure observed but of very poor quality.

Trial no. 4:

We changed the temperature from 800 to 860° C and kept all other conditions same.

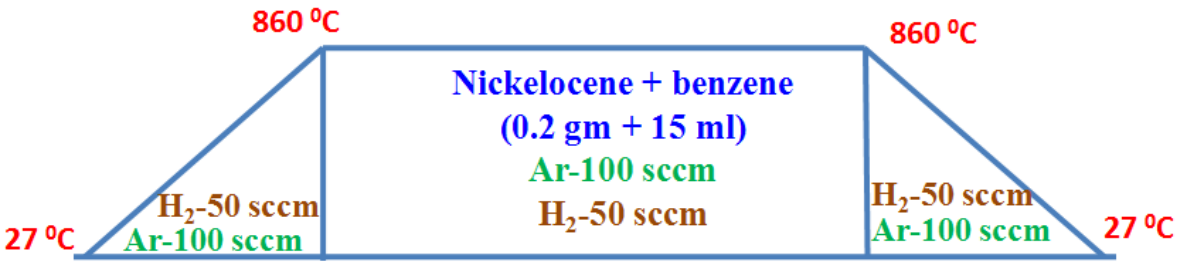

Fig.3.5: Flow diagram of entire experimental process

Result: Sample obtained like black powder and after characterizationNickle filled CNT like structure is observed .

Chapter 4 Methods of characterization

Characterization techniques are referred to those methods through which one can identify an as-prepared sample with respect to its morphology, surface topology, internal structure, composition, etc. The characterization techniques used to study a sample, depends on its properties, features, tolerance to the imposed environment so that during the process, no damage is done to the sample either internally or externally.

In order to analyse the as-grown CNTs samples, a few tools capable of characterizing them at a microscopic and below scale were necessary as the crystal compound growths were expected to be up to several nanometres in size. On account of the focus upon streamlining the growth process and thereby, obtaining single dimension growths, the following powerful techniques of characterizing the samples were necessitated. The set up and working of these techniques are briefly summarized below:

4.1 X-Ray Diffraction (XRD):

It uses the spatial distribution and intensities of X-ray radiation scattered by the sample under study and helps in the investigation of the structure of the sample. X-ray diffraction analysis technique has been used successfully to establish the atomic crystalline samples because crystals have a rigid periodicity in structure and constitutes naturally produced diffraction gratings for X rays. When X radiation interacts with the electrons of a sample, the X rays are diffracted accordingly. The pattern of the diffraction depends on the wavelength of the X rays employed and on the structure of the object.

Crystals can be understood as regular arrays of atoms, and X-rays are considered as waves of electromagnetic radiation. Atoms scatter X-ray waves, mostly through the atoms' electrons. Just as an sea wave striking a beach lighthouse produces secondary circular waves emerging from the lighthouse, so an X-ray striking the electron produces secondary spherical wavesemerging from the electron. This phenomenon is called as elastic scattering, and the electron (or lighthouse) is called as the *scatterer*. A regular array of such scatterers produces a regular array of spherical in nature waves. Even though these waves cancel one another out in most of the directions through destructive interference, they might add constructively in a few specific directions, and that is determined by Bragg's law. X-ray scattering is a kind of elastic scattering; so the outgoing X-rays have the same energy, and hence the same

wavelength, as the incoming X-rays, only with changed direction. These specific directions can be seen as spots on the diffraction pattern called *reflections*.

Hence, X-ray diffraction results from an electromagnetic wave (the X-ray) impinging on a regular array of scatters (the repeated arrangement of atoms within the crystal).X-rays are commonly used to produce the diffraction pattern and the reason is their wavelength λ which is typically the same order of magnitude (1–100 angstroms) as that of spacing *d* between planes in the sample's crystal. As the wavelength of x-ray is in the range with the lattice parameter of the crystals, diffractions might be happening when it interact with the sample's surface. According to the Bragg law, diffraction happens only if the stated condition is verified

$$2d\sin\theta = n\lambda$$

With particular incoming x-ray wavelength (λ), the diffraction angle (θ) is related to the planar distance of crystals (d), as shown in the figure below. Thus from the diffraction spectrum, the information crystal structure can be produced. One of the biggest advantage of XRD is that it is a non-destructive analytical method which can be used to identify phase as well as orientation, to determine structural properties, to measure the thickness of thin films, estimate the size of nanoparticles, etc.

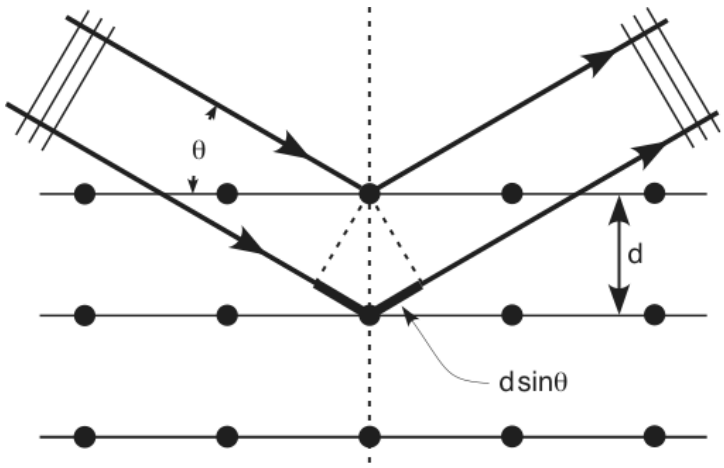

Fig.4.1:Bragg diffraction[25]

Fig. 4.2: Picture of XRD set up at Delhi Technological university

4.2 Scanning Electron Microscopy (SEM): It is a type of electron microscope that creates images of a sample by scanning the sample with a focused beam of electrons. The electrons interact with the sample's atom, producing manytypes of signals that can be detected and that contain information about the sample's surface topography and

composition. The electron beam is usually scanned in a raster scan pattern, and the position of the beam is combined with the detected signal to produce an image. SEM can achieve a very high resolution, even finer than 1 nanometer. The most used SEM mode is the detection of secondary electrons emitted by atoms which are excited by the electron beam. The amount of secondary electrons depends on the angle at which beam meets specimen surface, i.e. on specimen topography. By scanning the sample and by collecting the secondary electrons with the use of a special kind of detector, an image displaying the topographical information of the surface is formed, revealing minute details less than 1 nanometer in size[48].

SEM is typically consisted of the following features:
i)A source (electron gun) of the electron beam which is accelerated down the column.

ii) A series of lenses(objective and condenser) which act to control the diameter of the beam as well as to focus the beam on the specimen

iii) A series of apertures (micro scale holes in metal films) through which the beam passes and which affects properties of that beam.

iv) Controls for specimen position (x,y,z-height) as well as orientation (tilt, rotation);

v)An area of beam/interaction which generates several types of signals that can be detected and processed so as to produce an image or spectra; and

vi) All the above components are maintained at high vacuum levels.

Typically, in a SEM, an electron beam is thermionic in nature which is emitted from an electron gun that is equipped with a tungsten filament cathode. The electron beam, which has an energy generally ranging from 0.2 keV to 40 keV, is focused by one or may be two condenser lenses to a spot that is about 0.4 nm to 5 nm in diameter. The beam then passes through couple of scanning coils or pairs of deflector plate present in electron column, generally in the final lens, which then deflects the beam in the *x* and *y* axes in such a way that it scans in a raster fashion to cover a rectangular area of the sample's surface. The beam is rastered starting from left to right and from top to bottom. There is a direct one-to-one correspondence between the rastering pattern of the specimen and the rastering pattern that is being used to produce the image on monitor. The resolution chosen to image affects the number of pixels in each row as well as the total number of rows of the the scanned area. When primary beam of electrons interacts with the sample, the electrons loses their energy by

repeated random absorption and scattering within the interaction volume, which is normally less than 100 nm to approximately 5 μm into the surface. The types of signals produced by a SEM include back-scattered electrons (BSE), secondary electrons (SE), characteristic X-rays ,Auger electrons, light (cathode luminescence) (CL).

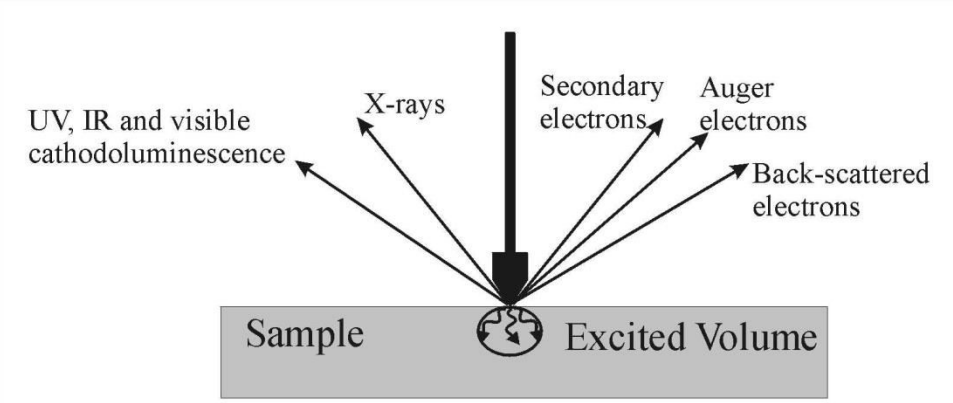

Fig. 4.3: Different types of electrons relesed during SEM images[24]

Fig. 4.4: Picture of SEM set up at Delhi technological University

1) Secondary Electrons: If an incident electron collides with an electron in a sample atom, it will knock that electron out of its orbital shell and the atom becomes ionized. Because the incident electron loses only a little energy during each collision, hence, multiple collisions are possible, continuing until the incident electron has no more energy to dislodge secondary

electrons. Each freed secondary electron has a small kinetic energy (<50 eV), and this energy is independent of the energy of the incident electron. If generated close enough to the sample surface (<10 nm), these secondary electrons can escape from the sample and can be collected by the detector. As a result, secondary electron imaging is closely related to sample topography[48].

2) Backscattered Electrons: If an incident electron collides with the nucleus of a surface atom, then the electron will bounce back or scatter 'backward' out of the sample as a backscattered electron (BSE). These electrons have high energies, typically in the range of 50 eV and that of the original incident electron. The production of these BSE electrons varies directly with atomic number, and thus backscattered electron images can be used in order to discern differences in sample atomic number[48].

3) Auger Electrons: As a result of generation of secondary electron, a vacancy is left in an ionized atom's electron shell. In order to fill this vacancy, an electron from a higher energy outer shell (from the same atom) can drop down to fill the vacancy. This creates a surplus energy in the atom that can be corrected by emitting an outer electron, which is an Auger electron. Auger electrons have a characteristic energy unique to the element from which they are emitted and hence, can be used to give compositional information about the target sample. However, Auger electrons have a relatively low kinetic energy and are only emitted from shallow sample depths (<3 nm)[48].

4) Characteristic X-rays: X-rays are also produced due to interactions of the incident electron beam with the sample's surface. Just like the Auger electron generating process, the excess energy produced as a result of reshuffling electrons to fill shell vacancies can also be emitted in the form of an X-ray rather than an Auger electron. X-rays have a characteristic energy unique to the element from which they are emitted and so provide compositional information about the sample.

4.3 Transmission Electron Microscopy (TEM) :

It is a microscopy technique in which the beam of electrons is made to transmit through an very thin specimen, interacting with the specimen as it passes through it. An

image is then formed by the interaction of the electrons which transmitted through the specimen, then the image is magnified and focused onto an imaging device, like a fluorescent screen, or on a layer of photographic film, or it can be detected by the use of a sensor. TEMs are capable of imaging at a much higher resolution than optical microscopes, due to the small de Broglie wavelength of the electrons. At smaller magnifications TEM image contrast is because of absorption of electrons in the material, or due to the thickness and composition of the material. At much higher magnifications complex wave interactions modulate the intensity of the produced image, requiring professional analysis of observed images. Alternate modes of use allow the TEM to observe modulations in crystal orientation, electronic structure, chemical identity and sample induced electron phase shift and the regular absorption based imaging. TEM forms a important analysis methodology in a range of scientific fields, in both physical as well as biological sciences. Transmission electron microscopy (TEM) uses very high energy electrons to penetrate through an ultrathin (≤100 nm) sample. This can increase spatial resolution in imaging (down to individual atoms) and the possibility of carrying out diffraction from nano-sized volumes. When electrons are accelerated up to a high energy levels (few hundreds keV) and focused onto a material, they can scatter or might backscatter elastically or inelastically, or even produce many interactions, source of different signals such as X-rays, Auger electrons or light. Some of them can be used in transmission electron microscopy (TEM)[47].

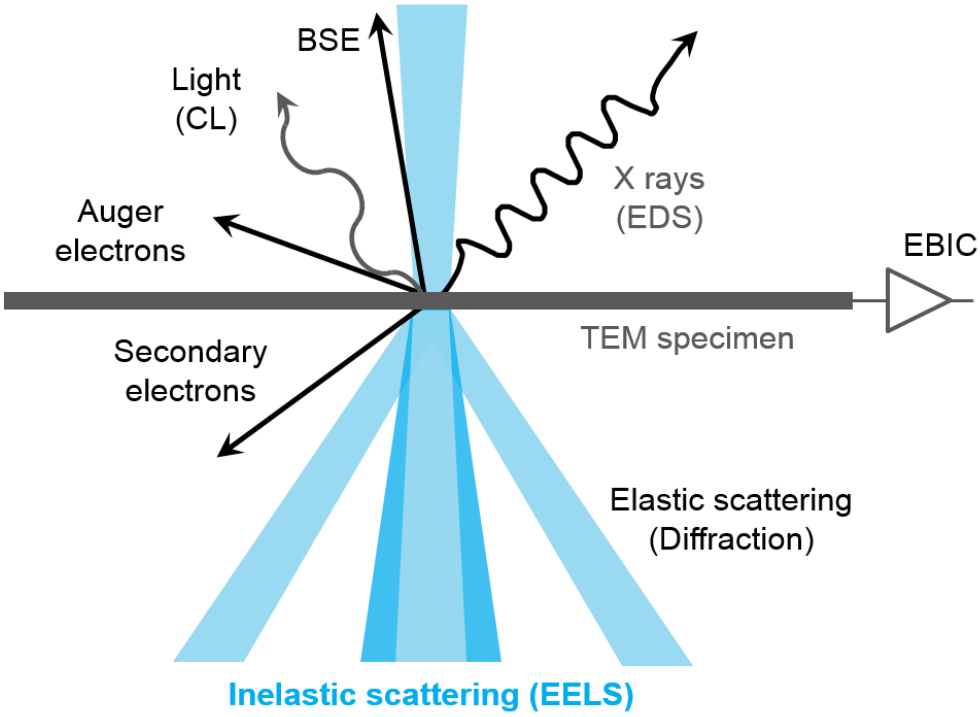

Fig. 4.5: Different types of signals produced during TEM imaging

Like all other matter, electrons have both wave as well as particle properties (as theorized by Louis-Victor de Broglie), and their wave like properties means that a beam of electrons can behave like a beam of electromagnetic radiation. The wavelength of electrons is directly related to their kinetic energy via the de Broglie equation. An additional correction must be made here to account for relativistic effects, as in a TEM an electron's velocity reaches very close to the speed of light, *c*.

$$\lambda_e \approx \frac{h}{\sqrt{2m_0E(1+\frac{E}{2m_0c^2})}} \qquad (4.1)$$

where, *h* is Planck's constant, *E* is the energy of the accelerated electron and *m*0 is the rest mass of an electron. Electrons are generally generated in an electron microscope by a particular process known as thermionic emission from a filament, commonly tungsten, in the same manner as that of a light bulb, or by field electron emission. The electrons are then accelerated using an electric voltage and focused by electrostatic as well as by electromagnetic lenses to the sample. The transmitted beam consists information about phase, electron density and periodicity; this beam is used to form the image[47].

TEM operates mainly in two modes, namely,

(A) Imaging Mode
(B) Diffraction Mode

A transmission electron microscope is made up of:

(1) Two or three condenser lenses to focus the electron beam onto the sample,
(2) An objective lens in order to form the diffraction in the back focal plane and the image of the sample on the image plane,
(3) Some intermediate lenses to magnify the image or the diffraction pattern on the screen.

(A) Imaging mode

If the sample is thin (< 200 nm) and made up of early periodic table chemical elements, the image presents a very low contrast when it is focused. To get an amplitude contrasted image, an objective diaphragm has to be inserted in the back focal plane to select the transmitted beam (and possibly few diffracted beam): the crystalline parts in Bragg orientation appears to be dark and not Bragg oriented parts or the amorphous appear bright. This type of imaging mode is called *bright field* mode BF. If the diffraction is made up of many diffracting phases, each of them can individually be differentiated by selecting one of its diffracted beams withthe help of objective diaphragm. To do so, the incident beam must be angled so that the diffracted beam is put on the objective lens axis to avoid off axis aberrations . This mode is known as *dark field* mode DF.The bright field and dark field modes are used for imaging materials to nanometer scale[48].

Fig. 4.6: Picture of TEM @ Institute of Physics, Bhubaneswar

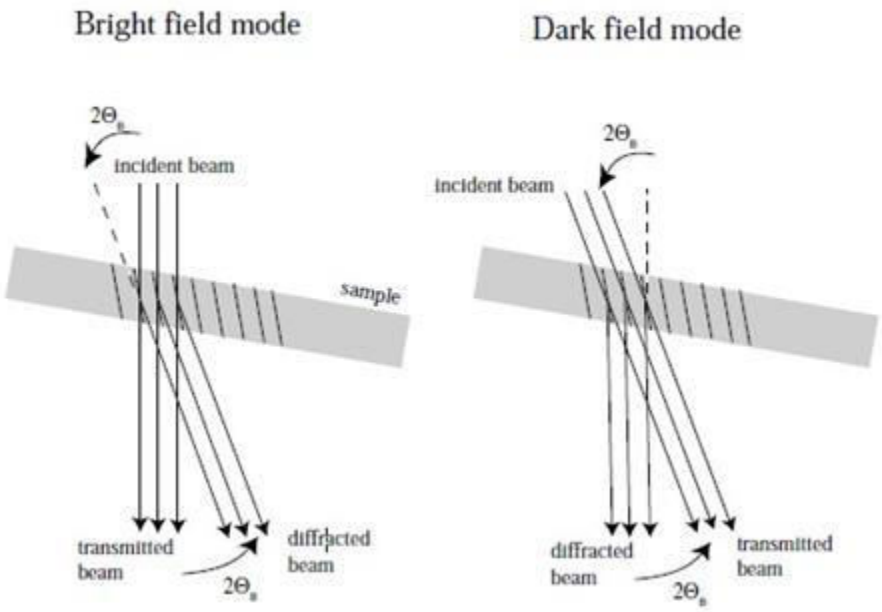

Fig. 4.7: Bright and dark field modes for imaging[21]

(B) Diffraction Modes:

The selected area diaphragm is used only to select one part of imaged sample for example a particle or a precipitate. This mode is known as selected area diffraction SAED. The spherical aberrations of the objective lens restrict the area of the selected object to few hundreds of nanometers. However, it is possible to obtain diffraction patterns of a smaller object by focusing the electron beam with the projector lenses to obtain a small spot size on the object surface (2-10 nm). The spots of SAED become disks whose radii depend on the condenser diaphragm. This is called microdiffraction.

SAED and microdiffraction patterns of a crystal permit to obtain the symmetry of its lattice and calculate its interplanar distances (with the Bragg law). This is useful to confirm the identification of a phase, after assumptions generally based on the literature of the studied system and on chemical analyses[48].

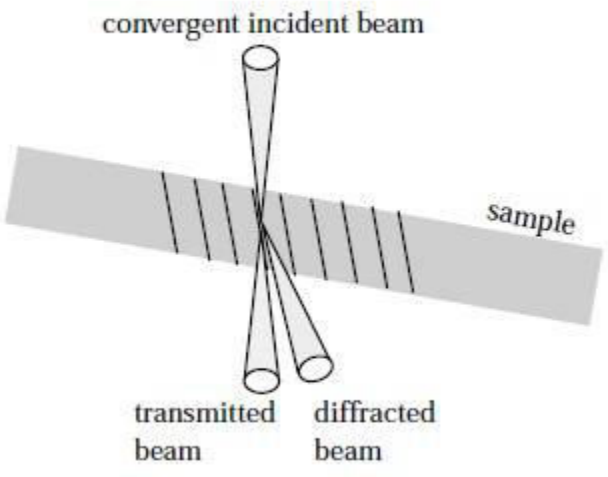

Fig. 4.8: Diffraction Mode[22]

4.4 Thermo gravimetric Analysis :

Thermo gravimetric analysis (TGA) is a method of thermal analysis in which changes in physical and chemical properties of materials are measured as a function of increasing temperature (with constant heating rate),or as a function of time (with constant temperature and/or constant mass loss). TGA can provide information about physical phenomena,such as second order phase transitions, including vapor transitions,including vaporization,sublimation,absorption,adsorption and desorption. Likewise,TGA can provide information about chemical phenomena including chemisorptions,desolvation (especially dehydration),decompostion, and solid-gas reactions(e.g.,oxidation or reduction).

TGA is commonly used to determine selected characteristics of materials that exhibit either mass loss or gain due to decompostiton,oxidation,or loss of volatiles(such as moisture)[46].

Fig. 4.9: Picture of Thermo gravimetric Analysis (TGA) instrument

Common appliations of TGA are:

(1) Materials characterization through analysis of characteristic decomposition patterns.

(2) Studies of degradation mechanisms and reaction kinetics.

(3) Determination of organic content in sample.

(4) Determination of inorganic (e.g. Ash) content in a sample , which may be useful for corroborating predicted material structures or simply used as chemical analysis.

It is an especially useful technique for the study of polymeric materials.including thermoplastics,thermosets,elastomers,composites,plastic films,fibers,coatings and paints. Discussion of the TGA aparatus,methods,and trace analysis will be elaborated upon below.Thermal stability,oxidation,and combustion,all of which are possible interpretaions of TGA traces,will also be discussed.

Thermogarvimetric analysis (TGA) relies on a high degree of precision in three measurements: mass change, temparature and temperature change. Therefore, the basic instrumental requirements for TGA are a precision balance with a pan loaded with the sample, and a programmable furnace.The furnace canbe programmed either for aconstant heating rate ,or for heating to acquire a constat mass loss with time[46].

Though a constant heating rate is more common, a constant mass loss rate can illuminate specific reaction kinetics.For example,the kinetic parameters of the carbonization of polyvinyl butyral were found using a constant mass loss rate 0.2 wt %/min. Regardless of the furnace programming,the sample is placed in a small,electrically heated furnace equiped with a thermocouple to monitor accurate measurements of the temperature by comparing its voltage output with that of voltage versus temperature table stored in the computers's memory. A reference may be placed on another balance in a seaparte chamber. The atmosphere in the sample chamber may be purged with an inert gas to prevent oxidation or other indesired reactions. A different process using a quartz crystal microbalance has been devised for measuring smaller samples on the order of a microgram[46].

The TGA instrument continuously weighs a sample as it is heated to temperatures of up to 2000 °C for coupling with FTIR and Mass spectroscopy gas analysis. As the temperature increases, various components of the sample are decomposed and the weight percentage of each resulting mass change can be measured. Results are plotted with temperature on the X-axis and mass loss on the Y-axis. The data can be adjusted using curve smoothing and first derivatives are often also plotted to determine points of inflection for more in-depth interpretations[46].

If the identity of the product after heating is known, then the ceramic yield can be found from analysis of the ash content (see discussion below). By taking the weight of the known product and dividing it by the initial mass of the starting material, the mass percentage of all inclusions can be found. Knowing the mass of the starting material and the total mass of inclusions, such as ligands, structural defects, or side-products of reaction, which are

liberated upon heating, the stoichiometric ratio can be used to calculate the percent mass of the substance in a sample. The results from thermogravimetric analysis may be presented by

(1) Mass versus temperature (or time) curve, referred to as thethermogravimetric curve.

(2) Rate of mass loss versus temperature curve, referred to as the differential thermo gravimetric curve.

Though this is by no means an exhaustive list, simple thermogravimetric curves may contain the following features:

- A horizontal portion, or plateau that indicates constant sample weight
- A curved portion; the steepness of the curve indicates the rate of mass loss
- An inflection (at which dw/dt is a minimum, but not zero)

Certain features in the TGA curve that are not readily seen can be more clearly discerned in the first derivative TGA curve. For example, any change in the rate of weight loss can immediately be seen in the first derivative TGA curve as a trough, or as a shoulder or tail to the peak, indicating two consecutive or overlapping reactions. Differential TGA curves also can show considerable similarity to differential thermal analysis (DTA) curves, which can permit easy comparisons to be made[46].

4.5 Raman spectroscopy :

This spectroscopic technique is generally used to observe vibrational , rotational, and some other low-frequency modes in a given system. Raman spectroscopy is usually used in chemistry to provide a fingerprint by which different molecules can be identified. It is a spectroscopic technique based on the inelastic scattering of monochromatic light unlike XRD, usually from a laser source. Here inelastic scattering means that the frequency of photons in monochromatic light changes upon interaction with the sample. Photons of the laser light are absorbed by the sample and then emitted. The frequency of the reemitted photons has a shift either in up or down direction when compared to the original monochromatic frequency, which is known as the Raman effect. This shift is capable of providing information about vibrational, rotational as well as other low frequency transitions in molecules. The Raman effect occurs due to inelastic scattering of photons by matter which may be solid, liquid or gas. This effect is observed as a shift in the frequency of the scattered light relative to the excitation frequency. These energy transitions are due to molecular vibrations. Because these vibrations consists identifiable functional groups, when energies of these transitions are plotted as in a spectrum, they can be used to identify the molecule[45].

A Raman system typically consists of four major components:

1. Excitation source (Laser).
2. Sample illumination system and light collection optics.
3. Wavelength selector (Filter or Spectrophotometer).
4. Detector (Photodiode array, PMT or CCD).

Typically, a sample is illuminated with the help of a laser beam. Electromagnetic radiations from the illuminated spot is collected with a lens and then sent through a monochromator. Elastic scattered radiation at wavelength corresponding to that of laser line (Rayleigh scattering) is filtered out, however the rest of the collected light is dispersed onto a detector by a notch filter or a band pass filter.

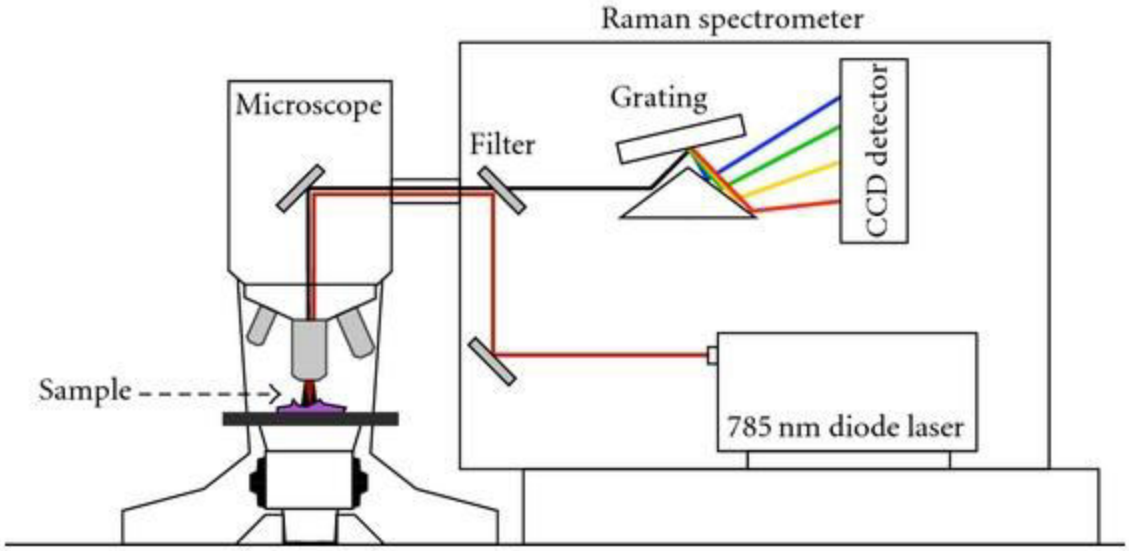

Fig. 4.10 : Schematic picture of Raman Spectrometer[27]

Raman shifts are generally reported in wave numbers, having units of inverse length, as this value is directly related to energy. In order to convert between spectral wavelength and wave numbers of shift in the Raman spectrum, the following formula is:

$$\Delta\omega \approx \left(\frac{1}{\lambda_{\circ}} - \frac{1}{\lambda_1}\right) \quad (4.2)$$

where is Δω the Raman shift expressed in wave number

λ_0 is the excitation wavelength and $\lambda_1$is the Raman spectrum wavelength.

The main advantages of Raman spectroscopy are its lack of sample preparation, high information content compatibility with aqueous systems, and non-destructive nature.

Chapter5 Results and Discussion

Structural characterizations:

Scanning electron microscopy:

As grown sample (scratched from quartz tube) was characterized by SEM to analysis their structure and morphology (as shown in Figure 5.1). As clear from the images MWCNTs are well separated and have tangled structure. The structure was found to be uniform throughout the sample. In order to further confirm the crystallinity and crystal structure, XRD has been performed on the sample.

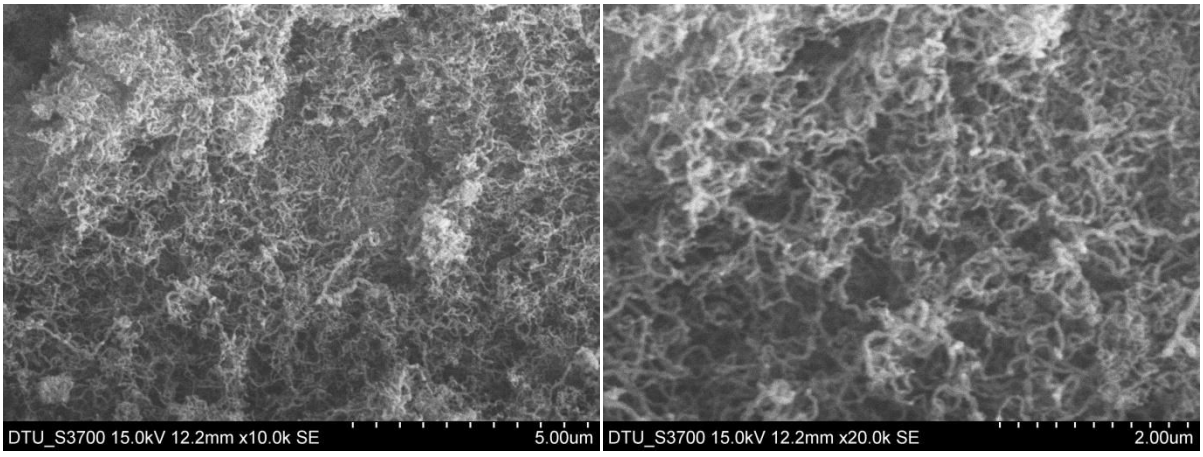

Fig. 5.1: SEM images of Ni-filled CNTs

X-ray diffraction:

X-ray diffraction (XRD) pattern is represented in Figure 5.2. Peak at 2θ =26.36° position has been identified assignature peak of MWCNT reflected from (002) plane of graphite (PCPDF 75-2078) was observed. Other diffraction peaks at 2θ = 44.63°,51.88° and 76.48° positions correspond to (111), (200) and (220) planes of the fcc Ni (PCPDF 87-0712). The FWHM of peak reflected from (111) plane is found to be 2°. The XRD analysis clearly indicated that CNT as well as filled Ni nanorods have good crystalline quality. The inter wall spacing of CNT wall has been calculated from XRD data which was found to be 3.37 Å.

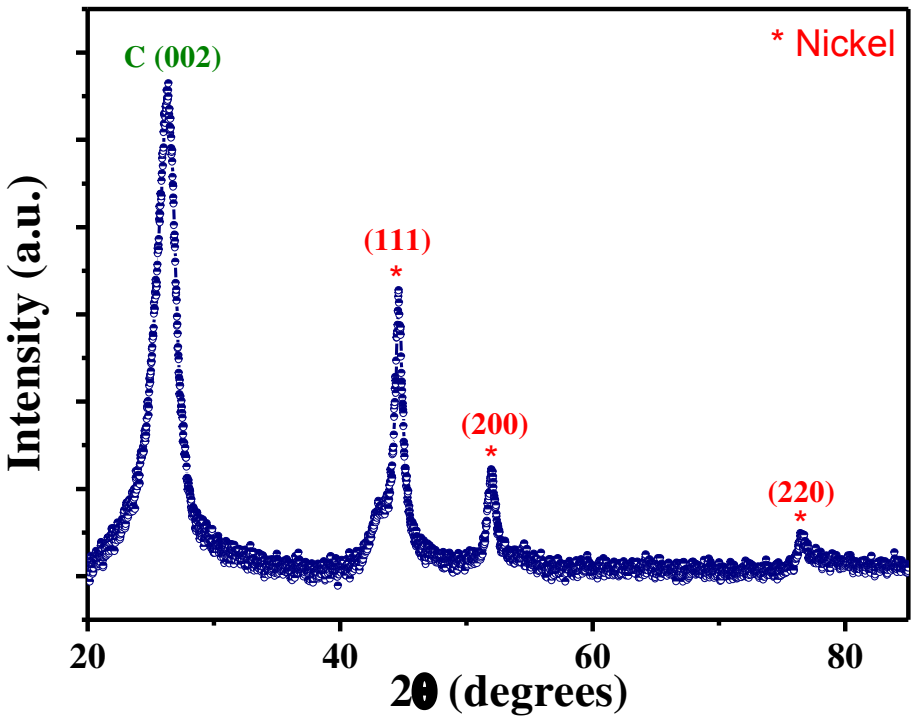

Fig. 5.2:X-Ray diffraction pattern

In order to confirm the filling of Ni inside the CNT, the sample was characterized with HRTEM (Figure 5.3). Figure 5.3 A shows the encapsulation of Ni nanorod inside the core of CNT and Fig. 5.3 B represent the close view of filled nanorod as well as lattice fringes of graphitic wall. The Outer diameter of the CNT was found to be 29.1 nm and diameter of inner core was 19.5 nm. The FFT generated on selected area of graphitic wall illustrates the inter wall spacing which was o to be 3.37 nm. This value is found to be in well agreement of that obtained by XRD analysis.

Transmission electron microscopy:

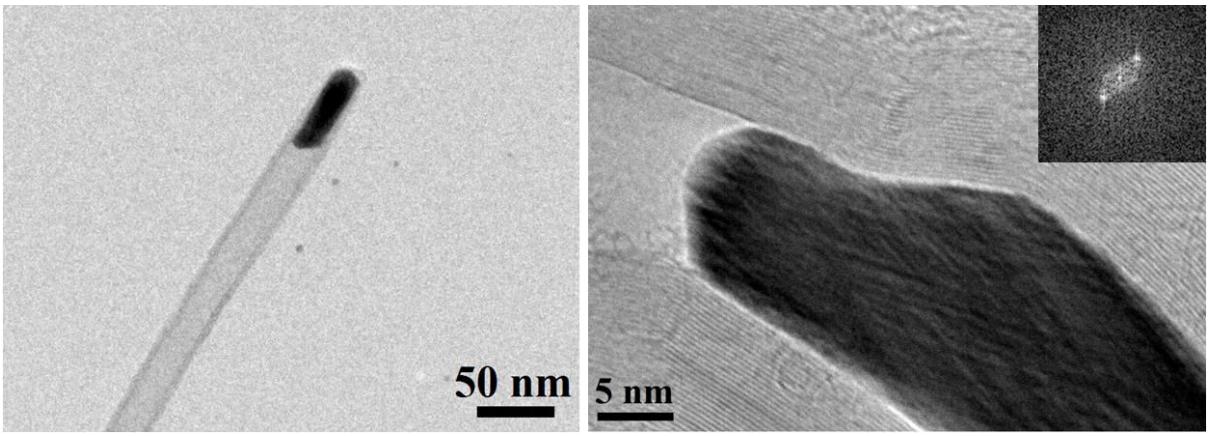

Fig. 5.3: TEM images of Ni-filled CNTs

Raman Spectroscopy:

In order to further investigate the structure properties, the as grown sample was characterized by Raman spectroscopy. Raman spectrum N-filled CNTs is shown in Figure 5.4. Main Raman features were observed at 1346 cm^{-1} and 1588 cm^{-1}. Peak at 1346 cm^{-1} is known as D band and it is associated with disorderness of the sample. Another peak at 1588 cm^{-1} is known as G band associated with graphitic structure.G-bandoriginates due to bond stretching vibration of pairs of sp^2 atoms aromatic rings of graphite. This band is a significance of quality of the graphitic structure where as D-band reflects the present of disorder. The ratio of these bands (I_g/I_d) reprsents the crystalline quality of the sample. In the present case it is to be found to be 0.81 which shows the good crystalline quality of CNT sample.

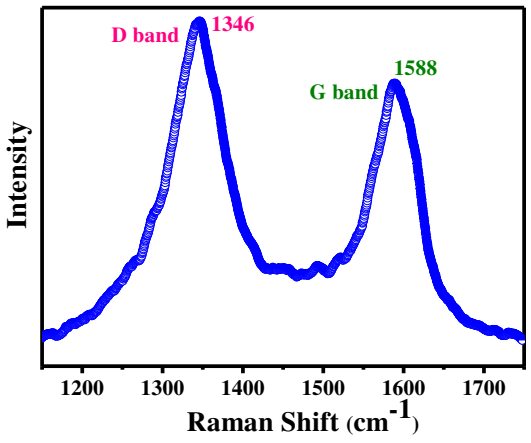

5.4: Raman spectrum of Ni-filled CNTs

Thermo gravimetric analysis:

Figures 5.5, show the TGA curves of as-grown Ni-filled MWCNT at heating rate of 5,10 and 15 ºC/min, respectively.The TGA curves clearly depict that here oxidation is a single step process. At the beginning of oxidation (from room temperature (RT) to 450 ºC) oxygen is adsorbed either on the surface of Ni-filled MWCNT or on bare catalytic impurities. Afterwards the amorphous carbon and filled-MWCNTs start to oxidize.Theonset temperatures i.e temperature at which as-grown sample of MWCNT started to oxidize were observed to be530ºC ,533°Cand 560ºC for 5,10and 15 ºC/min heating rates, respectively. At a heating rate of 5 ºC/min, the oxidationstarted early at a temperature of 530ºC. This reflects that the sample is less thermally stable at low heating rate as compared to higher heating rates at 10 °C and 15 ºC/min, where the oxidation started at 533°C,560°C respectively. From the TGA curves, it can be concluded that the onset temperatures of oxidation for different MWCNT samples lie in the range about 530 ºC – 560 ºC.

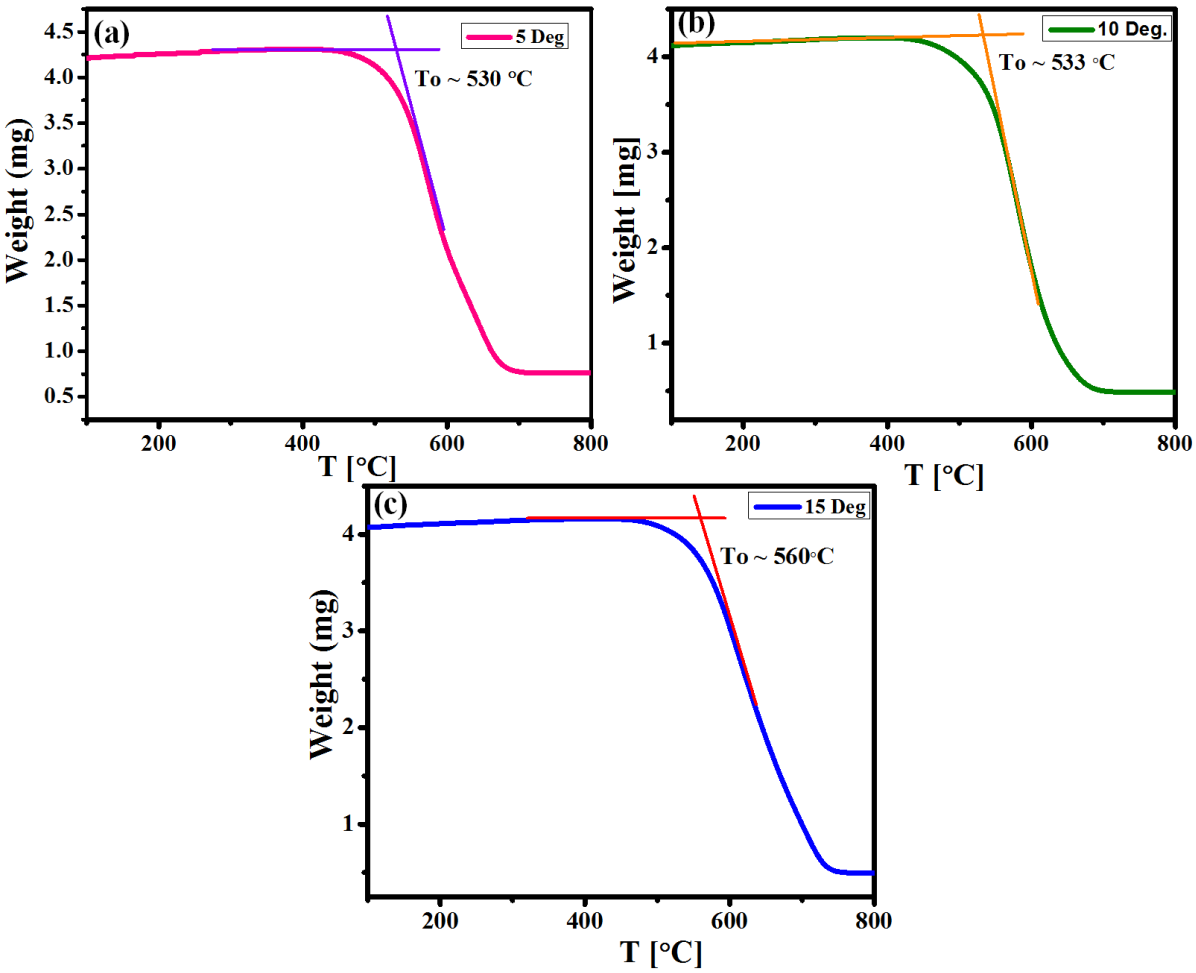

Fig 5.5: TGA Curves of as grown MWCNTs at different heating rate- (a) 5°C (b) 10°C (c) 15°C

The DTG curves plotted in Figures 5.6 indicate the weight change with respect to time at three heating rates of 5,10and 15 ºC/min, respectively. The initialization temperature is the temperature at which carbonaceous impurities start to decompose and the peak temperatures (T_p) as mentioned in DTG curves, is the oxidation temperature of MWCNT. In order to clearly identify the type of impurities present in the sample,the experimental data was fitted with Gaussian peaks. Four peaks appeared from the fitted curves and presumed to correspond to amorphous carbon, CNT and Carbon Onions respectively and demonstrated in Table 1.

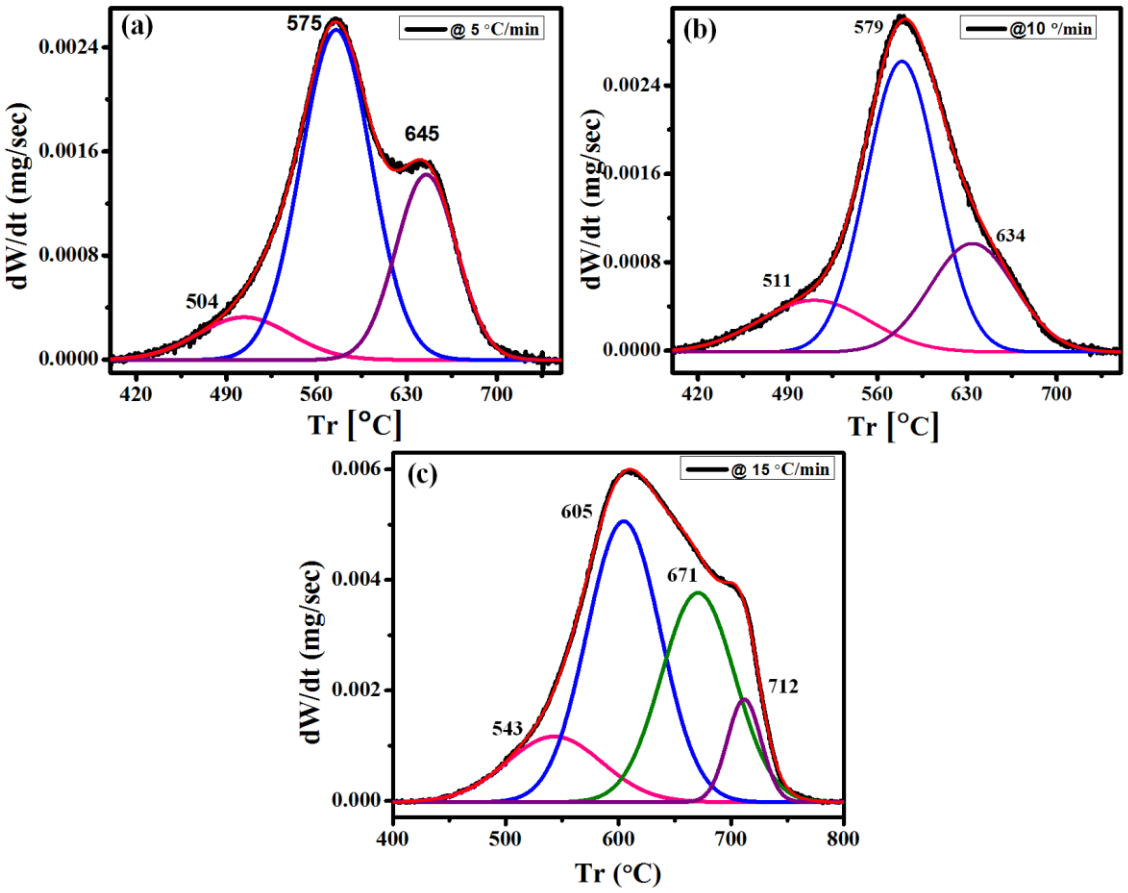

Fig 5.6: DTG Curves at different heating rates- (a) 5°C (b)10°C (c) 15°C

Heating Rate °C/min	Initialization Temperature [°C]				Oxidation Temperature T_P [°C]			
	Amorphous Carbon	CNTs		Carbon onions	Amorphous Carbon	CNTs		Carbon onions
5	424	494		582	504	575		645
10	418	500		547	511	579		634
15	448	CNTs of lower dia.	CNTs of higher dia.	676	543	CNTs of lower dia.	CNTs of higher dia.	712
		509	581			605	671	

Table 5.1: Initialization and oxidation temperature for various carbonaceous structures present in CNT sample.

Peaks were assigned by presuming the well-knownorder of thermal stability: amorphous carbon >SWCNTs > TWCNTs >MWCNTs.In the studied sample, T_P for TWCNTwas found to be nearly equal to the reported value for cobalt filled MWCNT .

The activation energies of sample have been calculatedby adopting the differential method for the three heating rates 5, 10 and 15 ºC/min. The equation (1) is used for the calculation of activation energy .

$$\ln\left(\frac{r}{W}\right) = E\left(-\frac{1}{RT}\right) + \ln A \qquad (5.1)$$

where, r is rate of change of weight with respect to time, W is weight and ln A is considered as constant. To calculate the activation energy, curves between ln (r/W) and 1/RT are plotted and shown in Figs. 3 (d), (e) and (f) for each impurity. The one side of the curve shows four regions of fitting; region-**I** for amorphous carbon, region-**II** for SWCNT, region-**III** for TWCNT, region-**IV** for MWCNT and other side region-**V** for catalyst. The values of the calculated activation energies are tabulated in Table 2.

Regions on the Graph / Heating Rate	**Region I Amorphous Carbon (eV)**	**Region II CNT (eV)**	**Region III Carbon onoions (eV)**	**Region IV Catalyst (eV)**
5 ºC/min	1.54	1.79	0.89	-5.78
10 ºC/min	2.07	1.06	1.89	-5.48
15 ºC/min	1.48	1.63	0.99	-8.50

Table 5.2: Activation energy calculated by adopting the differential method for carbonaceous structures at different heating rates

The activation energies have also been calculated by using Kissinger's corrected kinetic equation (integral method) . Kissinger's corrected kinetic equation is considered to be the most appropriate and is extensively applied for the kinetic study [35]. Kissinger's corrected kinetic equation is:

$$\ln\left(\frac{V}{T_P^2}\right) = \ln\left(\frac{AR}{E_a}\right) - \frac{E_a}{RT_P} \qquad (5.2)$$

where, V is heating rate (5, 10 and 15ºC/min),T_P is the peak temperature (K), E_a is the activation energy (kJ/mol), A is the pre exponential factor and R is the gas constant (8.314 J/mol K).

The activation energies can be calculated from the slope of the curve between ln (T_P^2/V) and 1/T_p, using equation (2) after substitution of the three different heating rates (5 and 15ºC/min) and the peak temperatures (T_p), keeping 1/T_P on the x-axis and ln (T_P^2/V) on the y-axis, using the formula:

$$Slope = \frac{E_a}{R} \quad (5.3)$$

$$E_a = Slope \times R \quad (5.4)$$

$$E_a = Slope \times 8.314 \times 10^{-3} \frac{KJ}{molK} \quad (5.5)$$

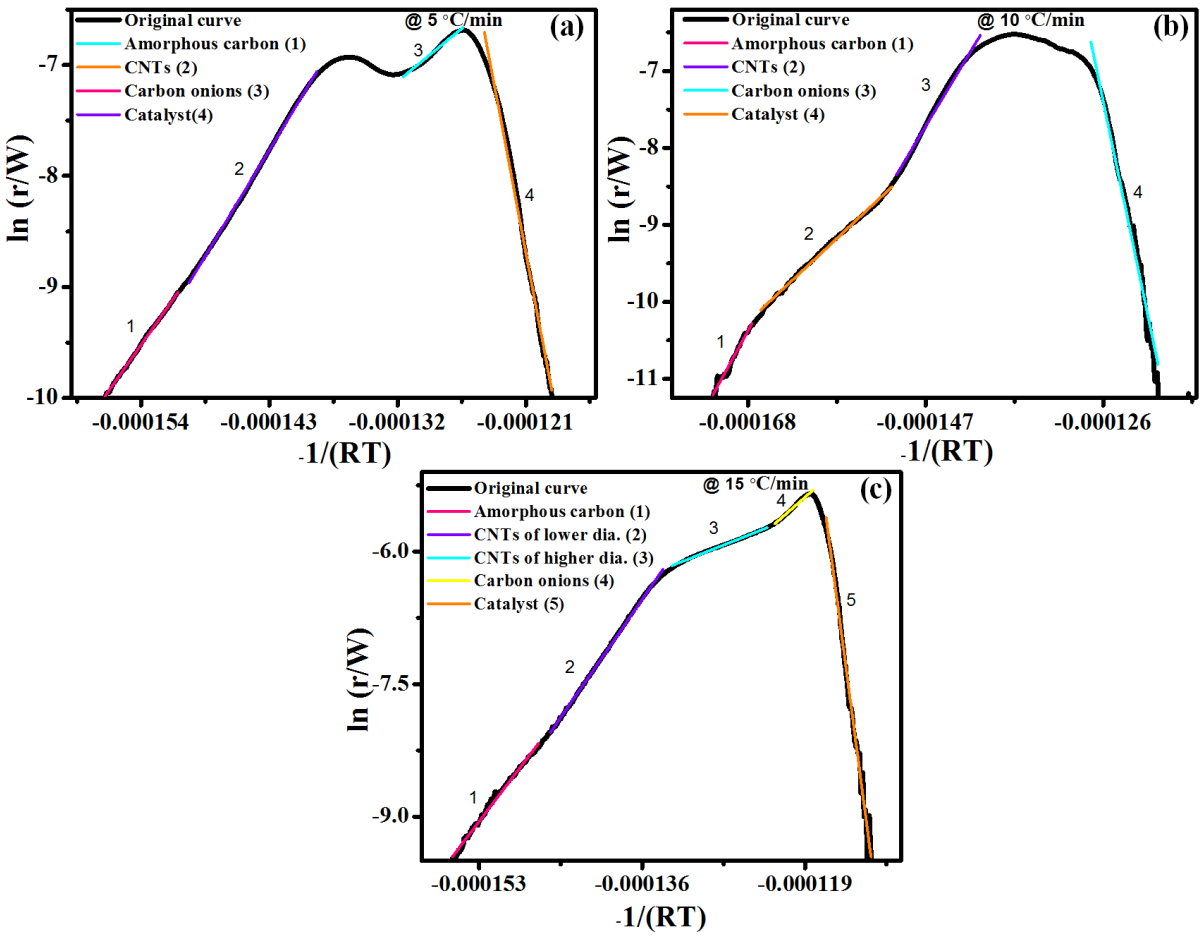

Fig 5.7: The four peaks mentioned in ascending order are assigned to the oxidation peaks of amorphous carbon, CNT, Carbon Onions at (a) 5°C,(b) 10°C,(c) 15°C

Solid line in the Fig. 5.8 depicts the experimental curve ln (T_P^2/V) vs 1/T_p and the fitted curves are represented by dotted line for four ranges of T_P.The activation energies for various carbonaceous structures, calculated from the slope using the equation (5), were found to be 0.47 ± 0.31 eV for amorphous carbon and activation energy for CNT is determined to be 0.77 ± 0.53 eV.

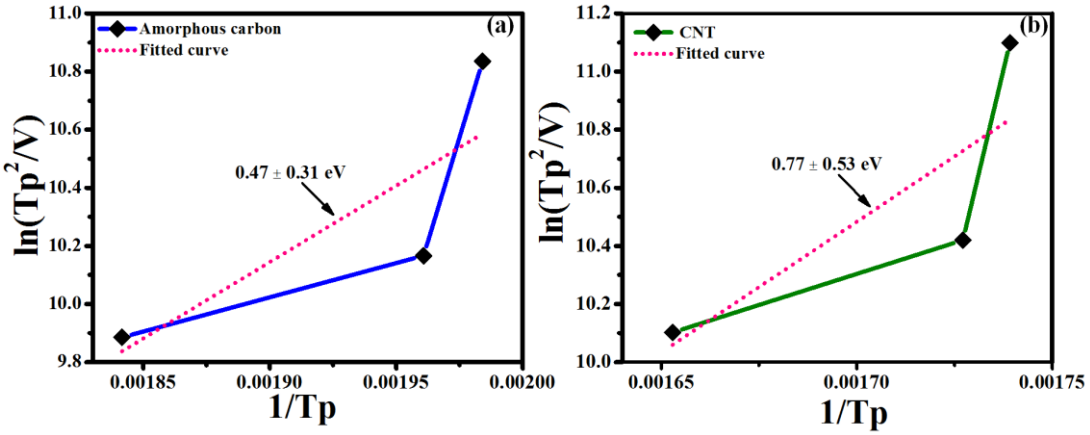

Fig 5.8:Kissinger's plot for activation energy- (a) amorphous carbon (b) CNT

As demonstrated above and in Figs 5.5, 5.6, 5.7 and 5.8 different structural forms of carbon have shown different oxidation behavior which may depend on the availability of reactive sites and defects. For example, amorphous carbon has been reported to oxidize at around 500 ºC due to the presence of a large number of active sites. In the present study, the observed value of oxidation temperature of filled-MWCNT (627 – 676 ºC), depending on the heating rate is in well agreement with the previously reported values (600 – 700 ºC) for the oxidation of graphitic structures.

A DSC curve plotted at heating rates 5, 10 and 15 ºC/min has been shown in Figure 5. From the curve it can be observed that the oxidation area is below the baseline according to Ref [44] it can be concluded that the oxidation process is endothermic and the peaks lies at 530 ºC,533°C and 560 ºC for the heating rates 5,10and 15 ºC/min, respectively as denoted in region I. In region I,upto 70% of the carbonaceous fractionsis oxidized.This further confirms that this endothermic oxidation is only of Ni-filled MWCNTs.

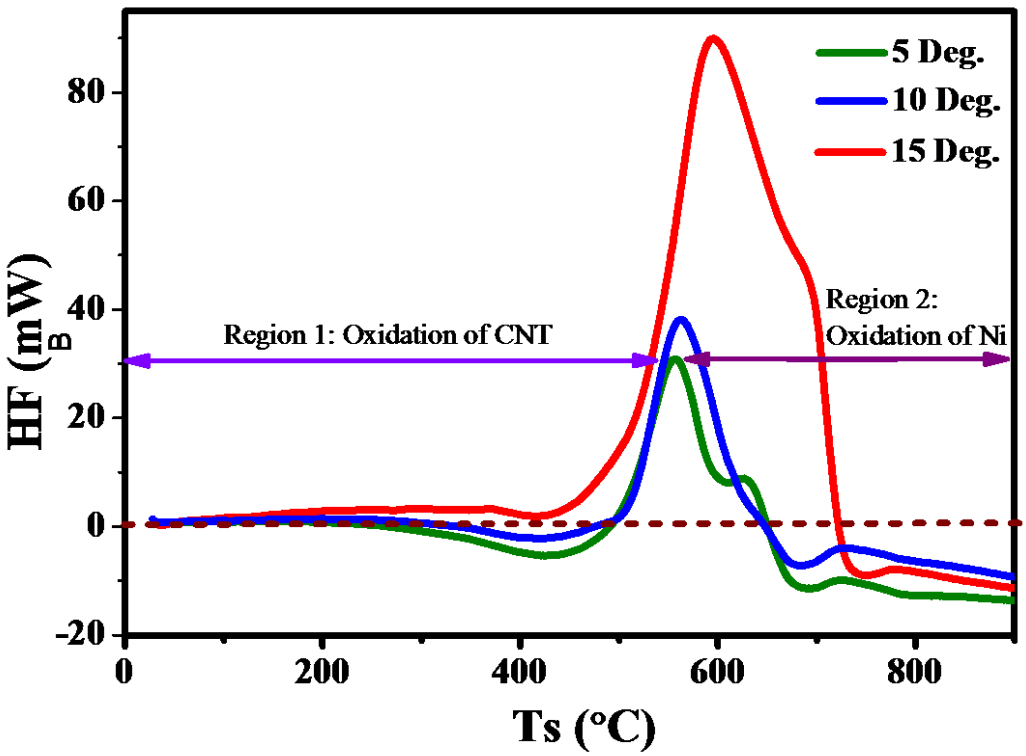

Fig 5.9: DSC curve for three different heating rates

Chapter 6 Conclusion

The aim of the project was to optimize the growth of Ni-encapsulated carbon nanotubes using thermal CVD and to make thero gravimetric analysis to find thermal stability and activation energies. Thermal chemical vapor deposition method was used as the synthesis route, with appropriate selection of precursors. In order to synthesize good quality of Ni-encapsulated carbon nanotubes, the synthesis conditions have been optimized to achieve the desired reproducible growth with large yield. The standard characterization techniques confirmed the quality and characteristics of the as-synthesized sample. A comparative TGA, DTG, and DSC studies of Ni-filled MWCNTs have been made for different heating rates. Ni-filled MWCNTs are found to have high thermal stability and high resistance to oxidation. The calculation of activation energy by adopting the Kissinger's Corrected kineticequation has been observed more accurately as compared to differential method. The detailed analysis of thermalstability and reactivity reveals that as-grown Ni-filled MWCNT have high purity and degree of graphitization A comparative DSC studyreveals that only the oxidation of Ni-filled MWCNT is endothermic.

References

1. Pawan K. Tyagi, M.K. Singh, AbhaMisra, UmeshPalnitkar, D.S. Misra, , E. Titus, N. Ali, G. Cabral, J. Gracio, M. Roy, S.K. Kulshreshtha , *Thin Solid Films,***2004**,*469–470*,127–130.

2. R Kumari, L Krishnia, V Kumar, S Singh, H K Singh, R K Kotnala,R RJuluri,U M Bhatta , P V Satyam , B S Yadav ,Z Naqvi ,P K Tyagi ,*Nanoscale*, **2016**, *8*,4299-310.

3. Lucky Krishnia,VinayKumar, ReetuKumari, PreetiGarg, Brajesh S. Yadav, AshutoshRath,ArnabGhosh, Ravindra K. Sinha, Manoj Kumar Singh, PawanK.Tyagi,*Advanced Science, Engineering and Medicine* ,**2016**,*8*:460-467.

4. Lucky Krishnia, ReetuKumari, Vinay Kumar, Anshika Singh, PreetiGarg, Brajesh S. Yadav, Pawan K. Tyagi,*Adv. Mater. Lett*.,**2016**,*7*, 230-234.

5. G. Che , B. B. Lakshmi , C. R. Martin , and E. R. Fisher ,*Chem. Mater.*, **1998**, *10*, 260–267.

6. Raja Shree Hirlekar, ManoharYamagar, HarshalGarse, MohitVij,VilasraoKadam,*Asian Journal of Pharmaceutical and Clinical Research,***2009**,*2*,17-27.

7. Uhland Weissker, SilkeHampel, Albrecht Leonhardt and Bernd Buchner, *Materials,***2010**, *3*, 4387-4427.

8. A. Leonhardt , M. Ritschel , R. Kozhuharova , A. Graff , T. Muhl , R. Huhle , I. Monch , D. Elefant , C.M. Schneidera, *Diamond and Related Materials*,**2003**,*12*, 790–793.

9. Martin Moskovits, Jing Li, Thomas L. Haslett, *Patent Publication no*.CA2310065 A1,**1999.**

10. GuzeliyaKorneva, Haihui Ye, YuryGogotsi, Derek Halverson, Gary Friedman, Jean-Claude Bradley, Konstantin G. Kornev, *NANOLETTERS*,**2005**,*5*,879-884.

11. www.nanocomptech.com/what-are-carbonnaotubes.

12. https://en.wikipedia.org/wiki/Nickelocene.

13. UhlandWeissker, SilkeHampel, Albrecht Leonhardt and Bernd B¨uchner, Carbon Nanotubes Filled with Ferromagnetic Materials.

14. UhlandWeissker, SilkeHampel, Albrecht Leonhardt and Bernd B¨uchner, Carbon Nanotubes Filled with Ferromagnetic Materials.
15. UhlandWeissker, SilkeHampel, Albrecht Leonhardt and Bernd B¨uchner, Carbon Nanotubes Filled with Ferromagnetic Materials.
16. UhlandWeissker, SilkeHampel, Albrecht Leonhardt and Bernd B¨uchner, Carbon Nanotubes Filled with Ferromagnetic Materials.
17. Uhland Weissker, SilkeHampel, Albrecht Leonhardt and Bernd B¨uchner, Carbon Nanotubes Filled with Ferromagnetic Materials.
18. Nanotechnology: practices and principles by sulbhakulkarni.
19. www.polyteknik.com/Laser-Ablation.
20. www.understandingnano.com/nanomaterial-synthesis-ball-milling.
21. Nanotechnology: Practices and principle by sulbhakulakarni.
22. Nanotechnology: Practices and principle by sulbhakulakarni.
23. https://jlk162.wordpress.com/2013/01/31/carbon-nanotubes-small-yet-mighty-engineering/.
24. http://www.porous-35.com/appendix-2.html,*Porous III-V Semiconductors by I. Tiginyanu, S. Langa, H. Föll and V. Ursachi.*
25. https://commons.wikimedia.org/wiki/File:Bragg_diffraction.png.
26. http://teachers.yale.edu/curriculum/viewer/initiative_10.05.07_u.
27. Lijing Ma, MaochangLiu,DengweiJinga, LiejinGuo, *J. Mater. Chem. A*, **2015**,*3*, 5701-5707.
28. http://courses.cs.washington.edu/courses/csep590a/08sp/projects/CarbonNanotubes,*By Chris Scoville, Robin Cole, Jason Hogg, Omar Farooque, and Archie Russell.*
29. Ali Eatemadi, HadisDaraee, HamzehKarimkhanloo, Mohammad Kouhi, NosratollahZarghami,AbolfazlAkbarzadeh,MozhganAbasi, YounesHanifehpour, Sang Woo Joocorresponding,*Nanoscale Res Lett*.,**2014**,*9*,393.
30. http://www.nanoscience.com/applications/education/overview/cnt-technology.
31. http://courses.cs.washington.edu/courses/csep590a/08sp/projects/CarbonNanotubes.
32. Ali Eatemadi, HadisDaraee, HamzehKarimkhanloo, Mohammad Kouhi, NosratollahZarghami,AbolfazlAkbarzadeh,MozhganAbasi, YounesHanifehpour, Sang Woo Joocorresponding,*Nanoscale Res Lett*.,**2014**,*9*,393.

33. http://courses.cs.washington.edu/courses/csep590a/08sp/projects/CarbonNanotubes.

34. http://www.iap.tuwien.ac.at/~gebeshuber/NT_bilder/10890790-C-3.

35. http://www.iap.tuwien.ac.at/~gebeshuber/NT_bilder/10890790-C-3.

36. http://www.nanowerk.com/nanotechnology/introduction/introduction_to_nanotechnology_26.

37. Muhammad Musaddique , Ali Rafique,JavedIqbal,*Journal of Encapsulation andAdsorption Sciences*, **2011**, *1*, 29-34.

38. http://www.nanowerk.com/nanotechnology/introduction/introduction_to_nanotechnology_22.

39. https://www.cheaptubes.com/carbon-nanotubes-101.

40. http://www.nanowerk.com/nanotechnology/introduction/introduction_to_nanotechnology_22.

41. Brajesh Kumar Kaushik and Manoj Kumar Majumder, *Carbon Nanotube Based VLSI Interconnects: Analysis and Desig,*Springer India,**2014**.

42. Uhland Weissker,SilkeHampel, Albrecht Leonhardt, Bernd Büchner, *Materials,***2010**, *3*, 4387-4427.

43. http://www.lakeshore.com/Documents/Magneticmedia/app/note.

44. Uhland Weissker,SilkeHampel, Albrecht Leonhardt, Bernd Büchner,*Materials,***2010**, *3*, 4387-4427.

45. https://www.scribd.com/document/270267382/Raman-Spectroscopy

46. http://nptel.ac.in/courses/115103030/23.

47. DissertationbyYangyangLi,*Characterization, Microstructure, and Dielectric properties of cubic pyrochlore structural $Bi_{1.5}MgNb_{1.5}O_7$ ceramics,*King Abdullah University of Science and Technology Thuwal Kingdom of Saudi Arabia,**2013**

48. DissertationbyYangyangLi,*Characterization, Microstructure, and Dielectric properties of cubic pyrochlore structural $Bi_{1.5}MgNb_{1.5}O_7$ ceramics,*King Abdullah University of Science and Technology Thuwal Kingdom of Saudi Arabia,**2013**

.